Aquatic Sciences (2024) 86:24
https://doi.org/10.1007/s00027-023-01039-6

Aquatic Sciences

RESEARCH ARTICLE

Dissolved greenhouse gas (CO_2, CH_4, and N_2O) emissions from highland lakes of the Andes cordillera in Northern Ecuador

Gonzalo Chiriboga[1,2] · Steven Bouillon[3] · Alberto V. Borges[1]

Received: 22 April 2023 / Accepted: 21 December 2023

Abstract

We report, in 15 Ecuadorian mountainous lakes, dissolved concentrations of CO_2, CH_4, and N_2O and a suite of ancillary biogeochemical variables (dissolved inorganic nutrients, oxygen, major cations, dissolved and particulate organic carbon, and the stable isotope composition of dissolved inorganic carbon and water). The sampled lakes were located in the páramos of Salve Facha and Antisana y Mojanda (northern region of Ecuadorian Andes), along an elevational gradient from 2213 to 4361 m above sea level, as well as a gradient of lake surface area (0.003–6.1 km^2) and depth (1–74 m). Most lakes were characterized by lower values of the partial pressure of CO_2 (pCO_2) (644–2152 ppm) than usually attributed to tropical lakes (~ 1900 ppm). Three lakes influenced by volcanic inputs were characterized by the highest pCO_2 values (3269–10,069 ppm), while two lakes bordered by large cities were characterized by the lowest pCO_2 values (208–254 ppm). Dissolved CH_4 concentrations ranged between 170 and 24,908 nmol/L and were negatively correlated to lake area and depth. N_2O saturation levels ranged between 64% and 101%. The surface waters were undersaturated in N_2O with respect to atmospheric equilibrium, probably due to inputs of soil–water with low N_2O levels owing to denitrification in soils. The data obtained in the sampled highland lakes was combined with published data from lowland lakes (elevation < 500 m, $n = 17$ for CO_2 and $n = 16$ for CH_4) to derive relations between CO_2 and CH_4 and lake surface area, allowing to compute CO_2 and CH_4 lacustrine emissions at the scale of the Amazon basin using the HydroLAKES spatial data set. The CO_2 and CH_4 emissions from highland lakes (elevation > 500 m) only represented 0.4% and 2% of the total lacustrine emissions at the scale of the Amazon basin, respectively. Total CO_2 and CH_4 emissions from lakes represented a small fraction (8.6%) of total lentic and lotic CO_2 and CH_4 emissions at the scale of the Amazon basin. The lake and river emissions of CH_4 represented ~ 3% of total CH_4 emissions from all compartments of the Amazon basin, mainly attributable to wetlands.

Keywords Amazon River · Ecuador · Mountainous lakes · CO_2 · CH_4 · N_2O

Introduction

Lakes and rivers are important components of the global carbon cycle in terms of transport and storage of organic carbon, as well as emissions of CO_2 and CH_4 to the atmosphere. Rivers transport from land to the ocean ~ 500 TgC/yr of organic carbon (Stallard 1998). The organic carbon buried in sediments of lakes (70–140 TgC/yr) is coequal to the rate in the oceans (120 TgC/yr), and comparable to the accumulation of organic carbon on land (soils and vegetation) during the last interglacial period (230 TgC/yr) (Cole 2013). This is striking because the total area of lakes is < 4% of the Earth's nonglaciated land area and ~ 1% of that of the oceans. Lakes and rivers also emit to the atmosphere CO_2 and CH_4, two potent greenhouse gases (GHGs). The CO_2 emission from lakes globally was estimated to ~ 300 TgC/yr (Raymond et al. 2013) and would be six times lower than that from rivers of ~ 1800 TgC/yr (Raymond et al. 2013; Liu et al. 2022). On the contrary, the emission of CH_4 from lakes (42 TgC/yr) could be approximately ten times higher than that from rivers (4.5 TgC/yr), accounting for 21% of total aquatic emissions, according to Rosentreter et al. (2021). The global CH_4 emission

✉ Alberto V. Borges
alberto.borges@uliege.be

1 Chemical Oceanography Unit, University of Liège, Liège, Belgium

2 Facultad de Ingeniería Química, Universidad Central del Ecuador, Ritter s/n y Bolivia, Quito, Ecuador

3 Department of Earth and Environmental Sciences, KU Leuven, Leuven, Belgium

Published online: 08 January 2024

from lakes has been recently revised downwards (31 TgC/yr) (Johnson et al. 2022) and that from rivers upwards (21 TgC/yr) (Rocher-Ros et al. 2023). The relative importance of CH_4 emissions from lakes compared with those from rivers at global scale is variable from one study to another, while at regional scale, some studies suggest that integrated CH_4 emissions from rivers might be higher than those from lakes, such as at the African continental scale (Borges et al. 2022). Yet, it is clear that the exchange of CO_2 and CH_4 between inland waters and the atmosphere is large enough to command further interest and research effort at the global scale. Further, a large source of uncertainty in the global CH_4 budget is attributed to emissions from inland waters (Saunois et al. 2020), thus, reducing the uncertainty of CH_4 emissions from lakes and rivers is clearly a priority (Johnson et al. 2022; Melack et al. 2022).

The uncertainty on the estimates of CO_2 and CH_4 emissions from lakes and rivers cannot be reduced by measurements alone, because it will be impossible to measure in situ GHG emissions in all rivers and lakes globally, given the global extent of river networks (~ 2×10^6 km by length and ~ 770,000 km^2 by area) (Allen and Pavelsky 2018) and of lakes (~ 1.4×10^6 lakes > 0.1 km^2 with a combined surface area of 2.7×10^6 km^2) (Messager et al. 2016). It is then required to model GHG emissions in rivers and lakes using either mechanistic models (e.g. Guo et al. 2020) or statistical relations with relevant predictors represented by spatial data sets. The choice of predictors needs to be anchored on a sound conceptual understanding of drivers of GHG emissions to minimize the application of spurious correlations and avoid redundancy in predictors of multivariate models. Numerous relevant potentially applicable spatial data sets are already available such as RiverATLAS (Linke et al. 2019) and HydroLAKES (Messager et al. 2016) and are expanding rapidly (Toming et al 2020; Altenau et al. 2021; Bonnema et al. 2022; Pi et al. 2022; Sikder et al. 2023). The most readily available predictors for lakes are morphometric, so regional or global upscaling attempts of CO_2 and CH_4 emissions from lakes have relied on lake surface area (Holgerson and Raymond 2016; Rosentreter et al. 2021) or depth (Borges et al. 2022). Others have integrated lake productivity based on statistical distributions of chlorophyll-a by lake size (DelSontro et al. 2018), although not accounting for strong latitudinal variations of productivity (Lewis 1987), or by integrating ecoclimatic zones (Johnson et al. 2022). So, there is an increasing need to expand and possibly standardize upscaling methods (Lauerwald et al. 2023). Yet, the largest limitation to reduce the uncertainty of the estimates of GHG emissions from rivers and lakes is the scarcity of field data of GHG emissions to adequately capture the very large spatial and temporal variability, allowing developing robust and reliable statistical models (e.g., Deemer and Holgerson 2021).

There are fewer studies of CO_2 and CH_4 variations in mountainous lakes than in lowland lakes. Available data suggest that there is no systematic difference in CH_4 emissions between mountainous and lowland lakes, while CO_2 emissions seem to be lower in mountainous lakes that occasionally act as sinks for atmospheric CO_2, based on data mainly collected in the Alps (Pighini et al. 2018), Rocky Mountains (McCrackin and Elser 2011; Crawford et al. 2015), Sierra Nevada (Cohen and Melack 2020), and the Tibetan Plateau (Yan et al. 2018, 2023; Wang et al. 2022). Available data sets of GHG emissions from lakes and rivers are also spatially skewed toward higher latitudes, mainly in North America and Scandinavia. These data sets cannot capture the features of GHG emissions from lakes and rivers in other parts of the globe with different climates and land cover. Yet, the majority of riverine GHG emissions are from the tropics (20 °N to 20 °S), ~ 60–80% for CO_2 (Raymond et al. 2013; Borges et al. 2015; Lauerwald et al. 2015; Sawakuchi et al. 2017; Liu et al. 2022) and ~ 50–70% for CH_4 (Sawakuchi et al. 2014; Rocher-Ros et al. 2023). Emissions from tropical lakes represent 37–50% of the total for CH_4 (Bastviken et al. 2011; Johnson et al. 2022) and 34% for CO_2 (Raymond et al. 2013). The estimate of emissions of CO_2 from tropical lakes as given in existing literature has been recently questioned and seems to have been overestimated (Borges et al. 2022). The CO_2 emissions from tropical lakes might, in fact, be lower than their counterparts at higher latitudes (Borges et al. 2022), while the CH_4 emissions from tropical lakes are disproportionately intense compared with their higher-latitude counterparts (Bastviken et al. 2011; Johnson et al. 2022; Borges et al. 2022). Relatively lower lacustrine CO_2 but higher lacustrine CH_4 emissions in tropical climates than at higher latitudes are partly related to high phytoplankton production in nonhumic lakes (Morana et al. 2023) that leads to the uptake of dissolved CO_2 but at the same time high CH_4 production in sediments (Borges et al. 2022) due to the deposition of fresh phytoplankton detritus (Grasset et al. 2018). Similarly, prior estimates of emissions of N_2O (Kroeze et al. 2010) from both rivers and lakes globally have been recently questioned and revised downwards (Hu et al. 2016; Maavara et al. 2019; Lauerwald et al. 2019). Even so, the N_2O emissions modeled from nitrogen deposition rates and emission factors (Lauerwald et al. 2019) seem to provide higher estimates in tropical lakes compared with those derived from field measurements (Borges et al. 2022). Additionally, emissions of N_2O from tropical lakes are lower compared with their boreal counterparts (Borges et al. 2022; 2023). This calls for a careful evaluation and a reduction of uncertainty of the GHG emissions from tropical lakes and rivers.

Until recently, the majority of research on GHG emissions from tropical inland waters was carried out in South America and in particular on the Amazon basin, as reviewed by Melack (2016) for CO_2, and Melack et al. (2022) for

CH_4. Melack et al. (2022) summarized published CH_4 fluxes and regional estimates in several types of aquatic systems (including rivers, lakes, reservoirs, and several types of wetlands), evaluated the adequacy of methods, and listed the limitations in current estimates. Melack et al. (2022) also identified regions or habitats of the Amazon basin with few or no data that include systems at altitudes above 500 m, mainly in the Andes cordillera. These systems are expected to be sensitive to climate change as increased air temperature accelerates the thawing of glaciers, leading to an increase in surface runoff (Bliss et al. 2014; LópezMoreno et al. 2014), that should affect GHG emissions from existing aquatic environments, as well as their coverage by the emergence of new lakes and ponds (Bosson et al. 2023).

Here, we report the dissolved concentrations of CO_2, CH_4 and N_2O in 15 lakes located in the northern region of Ecuadorian Andes along an elevational gradient from 2213 to 4361 m above sea level, as well as a gradient of lake surface area (0.003–6.1 km^2) and depth (0.9–74 m) (Fig. 1). Most lakes were located in the páramos of Salve Facha and Antisana y Mojanda. We also report a large suite of biogeochemical variables that allow us to characterize the lakes and provide some insights into the biogeochemical and physiographic drivers of the variability of GHGs in the sampled lakes, such as water temperature, specific conductivity, oxygen saturation level (%O_2), stable isotope composition of carbon (δ^{13}C-DIC) in dissolved inorganic carbon (DIC), nitrate (NO_3^-), nitrite (NO_2^-), ammonium (NH_4^+), total alkalinity (TA), major cations (Na^+, Mg^{2+}, Ca^{2+}, K^+), dissolved silicate (DSi), Fe, stable isotope composition of O and H of H_2O (δ^{18}O-H_2O and δ^2H-H_2O), and dissolved organic carbon (DOC) and particulate organic carbon (POC) concentrations. We explore modelling of CO_2 and CH_4 emissions to the atmosphere from the lakes using our data in highland lakes and literature data for lowland lakes (totaling about 30 lakes for each gas), statistical relations with relevant predictors from HydroLAKES (Messager et al. 2016), and recently published estimates of ebullitive CH_4 emissions (Borges et al. 2022). Finally, the upscaled lacustrine CO_2 and CH_4 emissions are compared with the emissions from rivers based on a recent estimate at the scale of the Amazon basin that included data from the mountainous Andean streams (Chiriboga and Borges 2023).

Material and methods

Site description

A vast amount of headwaters can be found in the Andes, which contribute 82% of sediments and solutes to the Amazon basin (McClain and Naiman 2008). Páramos are Andean mountain ecosystems that are located discontinuously in the Neotropics at elevations between 3000 m and up to 4300 m, mainly from Venezuela to northern Peru. The páramos occupy more than 30,000 km^2 in South America. Ecuador is the country with the highest proportion of its territory covered by páramos (with 7%) Páramo lakes constitute a primary source of drinking water for large populations in Ecuador, Colombia, and Venezuela. In Ecuador, the air temperature is relatively constant, the average annual rainfall is 1345 mm and occurs throughout most of the year; only ~ 12% of the days are dry. These conditions have favored the formation of peat and a large number of wetlands and lakes. The páramo usually presents deep and organic rich soils (30% by volume) and its vegetation is dominated by grasslands (Zapata et al. 2021).

Lake sampling

The lakes were sampled at different periods from April 2019 to March 2022, with an inflatable boat, during daytime (early morning to late afternoon), and using three strategies: (1) Lake Salve Fecha was sampled at a single location (close to the edge of the lake) during four occasions in 2019 and 2020 (1 April 2019, 1 September 2019, 1 October 2019, and 1

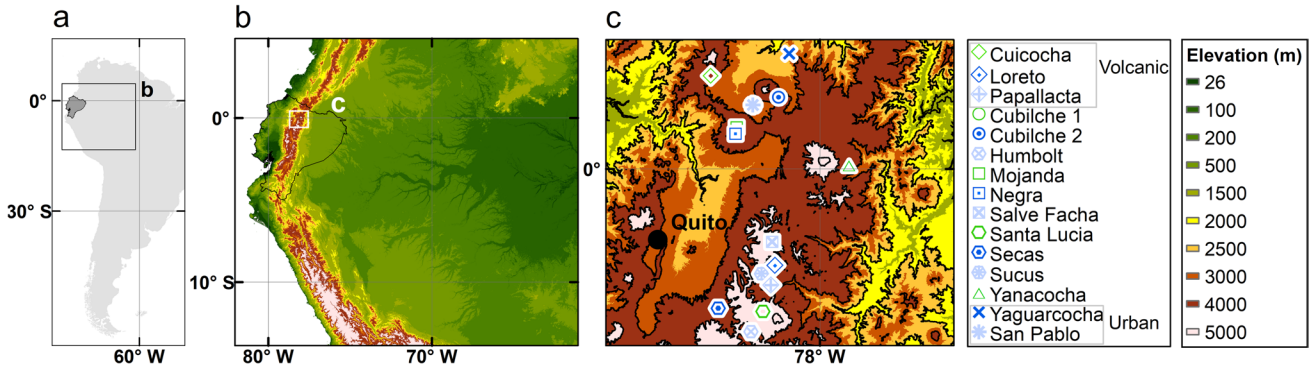

Fig. 1 Fifteen sampled highland lakes in Northern Ecuador

January 2019) as part of the sampling of the Napo river network (Chiriboga and Borges 2023); (2) Lakes Santa Lucía, Secas, and Humbolt were sampled on two occasions (24–25 September 2021 and 17–21 December 2021), along a transect across the longest length with equidistant points ($n=9$, 6, 3, respectively); (3) the remaining 11 lakes (Cubilche 1 and 2, Cuicocha, Loreto, Mojanda, Negra, Papallacta, San Pablo, Sucus, Yaguarcocha, and Yanacocha) were sampled at only one station in the center of the lake on one occasion, from 22 March 2022 to 28 March 2022. Admittedly, CO_2, CH_4 and N_2O in surface waters of lakes show variations in time (from subdaily to seasonal) and horizontally (from shore to the deepest part frequently in the center) (Fernandez et al. 2020; Ngochera and Bootsma 2020; Mandryk et al. 2021; Borges et al. 2022; Peacock et al. 2023), but a "one station in the center" snapshot survey of lakes has frequently been used to investigate broad geographical gradients as a function, for instance, of climate or catchment land cover (Juutinen et al. 2009; Finlay et al. 2010; Lapierre and del Giorgio 2012; Kortelainen et al. 2020; Casas-Ruiz et al. 2021; Rodríguez-Cardona et al. 2023). Albeit not optimal, the "one station in the center" snapshot survey approach is a tradeoff between the detail of the description of within lake horizontal/temporal variability and a broad description of geographical gradients, with typical resources allocated to sampling effort. A statistical summary [average ± standard deviation (st. dev.), coefficient of variation (CV), median, first quartile (Q1), second quartile (Q2), minimum–maximum range] of the partial pressure of CO_2 (pCO_2) and the dissolved CH_4 and N_2O concentrations in Lakes Salve Fecha, Santa Lucía, Secas, and and Humbolt is given in Table 1. The data collected in Lake Salve Facha provided an indication of the temporal variability (during four different sampling occasions) at a single site, while data collected in Lakes Santa Lucía, Secas, and Humbolt provided an indication of the spatial variability (multiple sampling points), although also integrating temporal variability (during two different sampling occasions). Despite a relatively important variability indicated by the minimum–maximum and Q1–Q3 range, the median and average values of the three gases tended to converge, except for Lake Humbolt, possibly because of a lower number of samples ($n=6$) (Lewis 1993). The CV indicated that CH_4 was more variable (35–89%) than pCO_2 (29–66%), while N_2O was the least variable (6–16%). The variability of the three GHGs, as given by the CV, was highest in the smallest lake (Humbolt).

Sample collection and analysis

Water temperature, specific conductivity, pH, and $\%O_2$ were measured in surface water with a YSI multiparameter probe (ProPlus). Water samples for CH_4 and N_2O analysis were collected in duplicate borosilicate serum bottles (Weathon; volume 40 mL) with a 2L polyethylene bottle with the bottom cut and fitted with a silicone tubing at the stopper (Abril et al. 2007), poisoned with 100 µL of a saturated solution of $HgCl_2$ and sealed with a butyl stopper and crimped with an aluminum cap. After overnight equilibration, measurements

Table 1 Statistical summary (average ± st. dev., coefficient of variation (CV), median, first quartile (Q1), second quartile (Q2), minimum–maximum) of CH_4 concentration (nmol/L; relative analytical precision ± 10.9%), partial pressure of CO_2 (pCO_2; ppm, relative analytical precision ± 5.2%), and N_2O concentration (nmol/L, relative analytical precision ± 5.8%) in lakes were multiple samplings were carried out (Salve Fecha, Santa Lucía, Secas, and Humbolt). SA, surface area

		n	Average ± st. dev	CV (%)	Median	Q1	Q3	Minimum	Maximum
Santa Lucía *	CH_4 (nmol/L)	18	1577 ± 961	61	1467	709	2081	49	3347
(SA of 0.039 km^2)	pCO_2 (ppm)	18	1193 ± 344	29	1121	1012	1385	672	1882
	N_2O (nmol/L)	18	6.3 ± 0.8	13	6.1	5.6	6.9	5.0	8.0
Secas **	CH_4 (nmol/L)	12	743 ± 562	76	711	270	1173	46	1842
(SA of 0.19 km^2)	pCO_2 (ppm)	12	667 ± 229	34	760	701	793	129	818
	N_2O (nmol/L)	12	6.0 ± 0.9	15	6.2	5.6	6.6	4.4	7.2
Humbolt ***	CH_4 (nmol/L)	6	2513 ± 2243	89	1388	1267	4634	110	5165
(SA of 0.0026 km^2)	pCO_2 (ppm)	6	1344 ± 888	66	704	692	2297	691	2336
	N_2O (nmol/L)	6	5.2 ± 0.8	16	5.7	4.4	5.8	4.2	5.9
Salve Facha ****	CH_4 (nmol/L)	4	178 ± 62	35	199	167	209	87	228
(SA of 1.2 km^2)	pCO_2 (ppm)	4	1570 ± 618	39	1862	1541	1891	644	1912
	N_2O (nmol/L)	4	7.5 ± 0.4	6	7.5	7.2	7.8	7.0	7.9

*24 September 2021 ($n=9$) 17 December 2021 ($n=9$)

**25 September 2021 ($n=6$) 21 December 2021 ($n=6$)

***25 September 2021 ($n=3$) 21 December 2021 ($n=3$)

****1 April 2019 ($n=1$) 1 July 2019 ($n=1$) 1 October 2019 ($n=1$) 1 January 2020 ($n=1$)

were made, on a headspace (Weiss 1981) (15 mL of high-purity N_2 into the 40 mL sample bottles), with a gas chromatograph (SRI 8610C) with a flame ionization detector for CH_4 and electron capture detector for N_2O calibrated with CH_4:N_2O:N_2 gas mixtures (Air Liquide Belgium) with mixing ratios of 1, 10, and 30 ppm for CH_4, and 0.2, 2.0, and 6.0 ppm for N_2O, with a precision of ± 10.9% for CH_4 and ± 5.8% for N_2O (based on duplicate samples).

The pCO_2 in the water was measured in the field with a Li-Cor Li-820 infrared gas analyzer based on the headspace technique from four 60-mL polypropylene syringes filled directly with surface water. A headspace of 30 mL was created with ambient air that was equilibrated in the syringe with 30 mL of water by vigorous shaking during 5 min. The water temperature after equilibration was measured immediately after injection of the headspace with a portable thermometer (Testo 925). The pCO_2 in the atmosphere was measured by injecting ambient air sampled with an additional polypropylene syringe. The Li-Cor Li-820 was calibrated with pure N_2 and CO_2:N_2 gas mixtures (Air Liquide Belgium) of 388, 804, 3707, and 8146 ppm. The final pCO_2 value was computed taking into account the partitioning of CO_2 between water and the headspace, as well as equilibrium with HCO_3^- (Dickson et al. 2007) using water temperature measured in situ, after equilibration, and TA. The precision of pCO_2 measurement was ± 5.2%.

The CO_2 concentration is expressed as partial pressure in parts per million (ppm) and as dissolved concentration for CH_4 (nmol/L). N_2O data are presented as percent of saturation level (%N_2O, where atmospheric equilibrium corresponds to 100%), computed from the global mean N_2O air mixing ratios (https://www.esrl.noaa.gov/gmd/hats/combined/N2O.html), using the Henry's constant (Weiss and Price 1980).

Samples for δ^{13}C-DIC were collected in 12-mL Exetainer vials (Labco) and poisoned with 50 µL of a saturated solution of $HgCl_2$. Prior to the analysis of δ^{13}C-DIC, a 2-mL helium headspace was created and 100 µL of phosphoric acid (H_3PO_4, 99%) was added in the vial to convert carbonate (CO_3^{2-}) and bicarbonate (HCO_3^-) ions to CO_2. After overnight equilibration, up to 1 mL of the headspace was injected with a gastight syringe into a coupled elemental analyser—IRMS (EA-IRMS, Thermo FlashHT or Carlo Erba EA1110 with DeltaV Advantage). Calibration was performed with certified standards (NBS-19 or IAEA-CO-1 and LSVEC). The obtained data were corrected for isotopic equilibration between dissolved and gaseous CO_2 (Gillikin and Bouillon (2007). Reproducibility of measurement based on duplicate injections was typically better than ± 0.2‰.

Water was collected in surface water with a 2-L polyethylene bottle, and a known volume was filtered through 47 mm diameter GF/F Whatman glass fibber filters. The filtrated water was collected and further filtered through polyethersulfone syringe encapsulated filters (0.2 µm porosity) for NO_3^-, NO_2^-, NH_4^+, TA, major elements (Na^+, Mg^{2+}, Ca^{2+}, and K^+), as well as DSi and Fe, δ^{18}O-H_2O, δ^2H-H_2O and DOC. An additional water filtration was made on 25 mm diameter GF/F Whatman glass fibber filters for POC analysis.

Water samples for nutrient analysis (NO_3^-, NO_2^-, and NH_4^+) were stored frozen (−20 °C) in 50-mL polypropylene vials. NO_3^- and NO_2^- were determined with the sulfanilamide colorimetric with the vanadium reduction method (American Public Health Association 1998), and NH_4^+ with the dichloroisocyanurate–salicylate–nitroprussiate colorimetric method (Standing committee of Analysts 1981). Detection limits were 0.3, 0.01, and 0.15 µmol/L for NH_4^+, NO_2^- and NO_3^-, respectively. Precisions were ± 0.02 µmol/L, ± 0.02 µmol/L, and ± 0.1 µmol/L for NH_4^+, NO_2^- and NO_3^-, respectively.

Samples for TA analysis were stored at ambient temperature in polyethylene 55-mL vials. TA was measured by open-cell titration with HCl 0.1 mol/L according to Gran (1952), and data quality was checked with certified reference material obtained from Andrew Dickson (Scripps Institution of Oceanography, University of California, San Diego, CA), with a typical reproducibility better than ± 3 µmol/kg. DIC was computed from TA and pCO_2 measurements using the carbonic acid dissociation constants for freshwater of Millero (1979) using the CO2sys package.

Samples for δ^{18}O-H_2O and were δ^2H-H_2O stored at ambient temperature in polypropylene 8-mL vials. δ^2H-H_2O was measured on H_2 gas derived from a high-temperature (1030 °C) Cr-based reactor by automated injections of water using a TriPlus autosampler on an elemental analyzer (Thermo Flash HT/EA; Thermo Finnigan) coupled to a continuous-flow isotope-ratio mass spectrometer (Delta V Advantage; Thermo Finnigan). δ^{18}O-H_2O values were measured on a Thermo GasBench II coupled to a Thermo Delta XP IRMS after equilibration with CO_2. The long-term uncertainty for standards was ± 0.1‰ for δ^{18}O and ± 2.0‰ for δ^2H-H_2O.

Samples for major elements were stored at ambient temperature in 20-mL scintillation vials and preserved with 50 µL of HNO_3 (65%). Major elements were measured with inductively coupled plasma MS (ICP-MS; Agilent 7700x) calibrated with SRM1640a from National Institute of Standards and Technology, TM-27.3 (lot 0412) and TMRain-04 (lot 0913) from Environment Canada, and SPS-SW2 Batch 130 from Spectrapure Standard. The limit of quantification that in this case also corresponds to the background equivalent concentration was 0.038 mg/L for Na^+, 0.005 mg/L for Mg^{2+}, 0.077 mg/L for K^+, 0.029 mg/L for Ca^{2+}, 0.185 mg/L for DSi, and 0.37 µg/L for Fe. The precision was ± 4.1% for Na^+, ± 3.8% for Mg^{2+}, ± 4.9% for K^+, ± 2.4% for Ca^{2+}, ± 5.8% for DSi, and ± 4.6% for Fe.

Samples for DOC analysis were stored at ambient temperature and in the dark in 40-mL brown borosilicate vials with polytetrafluoroethylene (PTFE) coated septa and poisoned with 50 µL of H_3PO_4 (85%). DOC concentration was measured with a wet oxidation total organic carbon analyzer (IO Analytical Aurora 1030W), with a typical reproducibility better than ± 5%.

Filters for POC analysis were decarbonated with HCl fumes for 4 h and dried before encapsulation into silver cups; POC was measured on an EA-IRMS (Thermo FlashHT with DeltaV Advantage), with a reproducibility better than ± 5%. Data were calibrated with certified (IAEA-600: caffeine) and in-house standards (leucine, tuna muscle tissue) that were previously calibrated versus certified standards.

Flux computations and upscaling

The dissolved concentrations of CO_2 and CH_4 were estimated for each of 12,549 lakes in HydroLAKES (Messager et al. 2016) from statistical relations as function of lake surface area (LSA), derived from our own data in Ecuadorian highland lakes and data available from literature in the floodplain lakes of the Central Amazon (Abril et al. 2013; Amaral et al. 2020; Barbosa et al. 2016; Mitchell et al. 2018). We excluded from the analysis reservoirs that represent 0.06% of lake counts ($n = 8$) and 11% of total lacustrine surface area (2773 km^2) in the HydroLAKES data set.

The pCO_2 (in ppm) was computed from two linear regressions as a function of LSA (in km^2) according to:

$$\log(pCO_2) = -0.1293(\pm 0.0346) \times \mathrm{LSA} + 3.063(\pm 0.073) \quad (r^2 = 0.58; p = 0.0039; n = 12)$$

for an elevation > 500 m (highlands), excluding three lakes (Cuicocha, Loreto, and Papallacta) and

$$\log(pCO_2) = -0.0003745(\pm 0.0001642) \times \mathrm{LSA} + 3.508(\pm 0.061) \quad (r^2 = 0.26; p = 0.0376; n = 17)$$

for an elevation < 500 m (lowlands).

The CH_4 (in nmol/L) was computed from a linear regression as function of LSA (in km^2) according to:

$$\log(CH_4) = -0.3753(\pm 0.0426) \times \log(\mathrm{LSA}) + 2.545(\pm 0.066) \quad (r^2 = 0.71; p < 0.0001; n = 34)$$

for both highland and lowland lakes.

The water temperature (WT in °C) was computed from the air temperature (AT in × 10 °C) from HydroLAKES, according to:

$$\log(\mathrm{WT}) = 0.002192(\pm 0.000069) \times \mathrm{AT} + 0.8905(\pm 0.0151) \quad (r^2 = 0.98; p < 0.0001; n = 23)$$

The flux of CO_2 (FCO_2) and CH_4 (FCH_4) between surface waters and the atmosphere was computed according to:

$$F = k \times \Delta G,$$

where k is the gas transfer velocity and ΔG is the air–water gradient of a given gas.

The k normalized to a Schmidt number (Sc) of 600 (k_{600} in cm/h) was derived from the parameterization as a function wind speed (Cole and Caraco 2018):

$$k_{600} = 2.07 + 0.215 \times u^{1.7},$$

where u is wind speed (m /s) that was extracted from WorldClim (Fick and Hijmans 2017) for each lake in HydroLAKES.

k_{600} was converted to k for the Sc at in situ temperature (Wanninkhof 1992) according to:

$$k = k_{600} \times (\mathrm{Sc}/600)^{-0.5}.$$

A Monte Carlo error analysis (10,000 iterations) was conducted by propagating errors in the slope and constant of the equations of the gas concentrations and WT (refer to above equations), an uncertainty of ± 65% and ± 40% on dissolved CH_4 concentration and pCO_2, respectively, to account for within-lake variability (based on Table 1), and an error of ± 30% for k_{600} based on the reported variability across different lakes of k at low wind speeds (Cole and Caraco 2018).

Results and discussion

We sampled 15 lakes in Ecuador along an elevational gradient (2213–4361 m) (Fig. 1). The surface area of the sampled lakes ranged between 0.003 and 6.1 km^2, and lakes at higher elevation tended to be smaller (Fig. 2). Lakes were generally shallow, with depths ranging between 0.9 and 72 m, with a tendency toward shallower lakes at higher elevation (Fig. 2). Lakes Cuicocha, Loreto, and Papallacta are crater lakes (hereafter referred to as "volcanic"), and the others are of glacial origin. Among the latter, San Pablo and Yaguarcocha are surrounded by the cities of Otavalo and Ibarra, respectively (hereafter referred to as "urban").

Water temperature ranged between 10.2 and 15.7 °C and followed a clear elevational gradient (Fig. 2). The specific conductivity in the sampled lakes was generally low (20–183 µS/cm), except for the two "urban" lakes (San Pablo and Yaguarcocha) (294–298 µS/cm) and the three "volcanic" lakes (Cuicocha, Loreto and Papallacta) (708–722 µS/cm) (Fig. 2). The conductivity of the three "volcanic" lakes was lower than in crater lakes in active volcanic systems in Ecuador characterized by conductivity values > 10,000 µS/cm (Inguaggiato et al. 2010; Melián et al. 2021). Conductivity was negatively related to elevation for the non-"volcanic"

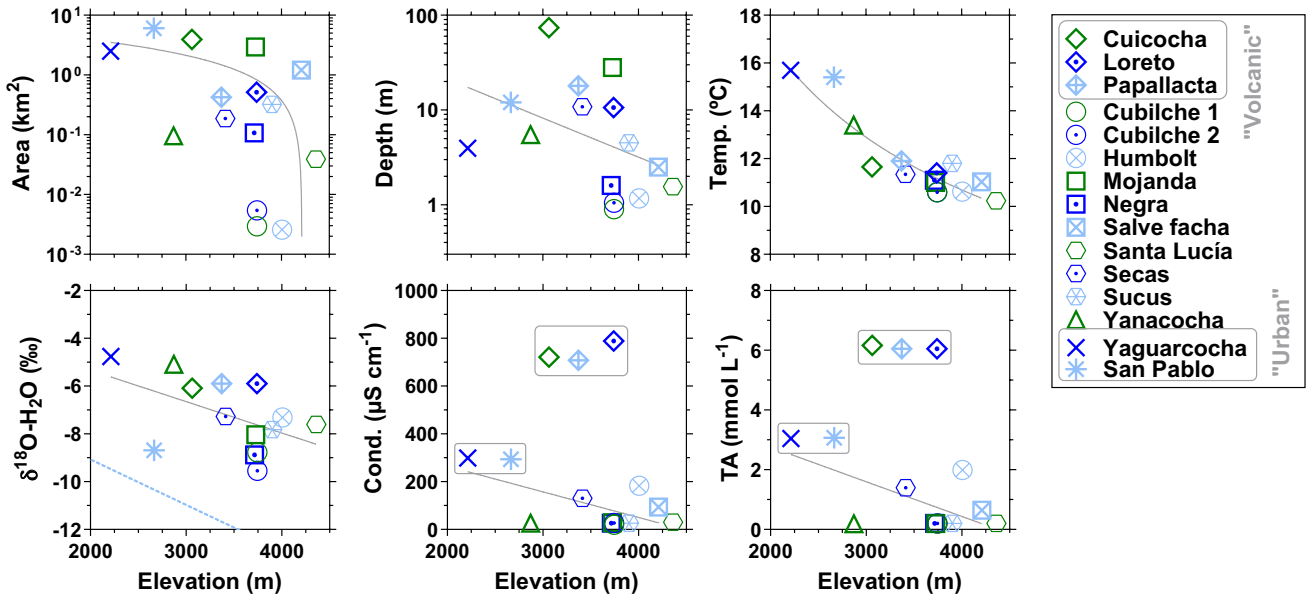

Fig. 2 Lake area (km^2), lake depth (m), water temperature (Temp. °C, analytical precision ± 0.1 °C), stable isotope composition of O of H_2O ($\delta^{18}O$-H_2O in ‰, analytical precision ± 0.1‰), specific conductivity (cond. µS/cm, analytical precision ± 0.1 µS/cm), and total alkalinity (TA in mmol/L, analytical precision ± 0.003 mmol/L) in surface waters of 15 highland lakes in Northern Ecuador (Fig. 1) versus elevation (m). Solid grey lines show fits to the data (Table S2). Dotted blue line indicates the $\delta^{18}O$-H_2O elevation gradient for Ecuador based on the global rain water isoscape given by Inguaggiato et al. (2010)

lakes, possibly reflecting the combination of decreasing lake size and temperature, and increasing soil organic matter content and precipitation with increasing elevation. In the Andean páramo, the soil organic carbon increases with elevation because of the decrease in temperature that leads to a decrease of organic matter mineralization in soils enhancing organic matter accumulation in soils (Poulenard et al. 2003). The high organic matter content of soils and lower temperature are not favorable to rock weathering leading to soil water with low mineral content (low conductivity). Additionally, high elevation páramo areas are characterized by high precipitation leading to dilution of solutes in surface waters, which should additionally contribute to decrease conductivity. TA showed very similar patterns to those of conductivity, with the three "volcanic" lakes characterized by higher TA values (6.05–6.16 mmol/L), followed by the two "urban" lakes (3.04–3.07 mmol/L), and the remaining lakes with the lowest TA values (0.19–1.99 mmol/L).

The cation sequence was dominated by Ca^{2+} or Na^+ followed by Mg^{2+} and K^+ (Table S1). The lakes with a high total cation content (21–147 mg/L and 1035–7916 µeq/L) were dominated by Na^+ ($Na^+ > Ca^{2+} > Mg^{2+} > K^+$), characteristic of sodium bicarbonate lakes. Lakes with a lower total cation content (~ 5 mg/L and ~ 235 µeq/L) were dominated by Ca^{2+} ($Ca^{2+} > Na^+ > Mg^{2+} > K^+$) (Table S1). This might indicate that the cation content of the sample lakes was related to the weathering of primarily volcanic rocks that dominate in the area (rhyolite, andesite, dacite, and diorite) (Mosquera et al. 2022). The three "volcanic" lakes (Cuicocha, Loreto, and Papallacta) were characterized by higher total cation content (144–147 mg/L 7778–7916 µeq/L) than the other 12 lakes (Table S1). The composition of the three "volcanic" lakes in divalent ions (Ca^{2+} and Mg^{2+}) relative to Na^+ was consistent with the other 12 lakes (Fig. S1). However, the three "volcanic" lakes had lower K^+, DSi and TA relative to the other 12 lakes (Fig. S1), which might possibly indicate different weathering mechanism in the three "volcanic" lakes compared with the other 12 lakes: either a noncongruent dissolution of aluminosilicate minerals or alternatively the weathering of a higher portion of sodium rich volcanic rocks in the three "volcanic" lakes compared with the other 12 lakes (Mosquera et al. 2022). The Fe content was negatively related to Na^+, and the three "volcanic" lakes had lower Fe relative to Na^+ compared with the other 12 lakes. This pattern might be possibly related to the chelation of Fe to dissolved organic matter, as Fe was correlated to DOC (Fig. S2).

The $\delta^{18}O$-H_2O values were negatively related to elevation and paralleled elevational gradient based on the global rain water isoscape (Inguaggiato et al. 2010) (Fig. 2). This might possibly indicate that the sampled lakes were mainly recharged by local precipitation (meteoric recharge). The offset between observed $\delta^{18}O$-H_2O values in the sampled lakes and the precipitation elevational gradient most probably resulted from fractionation during evaporation. The observed δ^2H and $\delta^{18}O$-H_2O values in the sampled lakes

deviated from the local meteoric water line (LMWL) (Inguaggiato et al. 2010), confirming substantial fractionation during evaporation (Fig. S3).

The DOC concentrations ranged between 1.2 and 12.8 mg/L, and DOC data points appeared to be grouped in clusters as a function of several variables such as elevation, lake area, lake depth, conductivity, and water temperature (Fig. 3). The three "volcanic" lakes (Cuicocha, Loreto, and Papallacta) were characterized by the lowest DOC concentrations (1.2–2.3 mg/L), the two "urban" lakes (San Pablo and Yaguarcocha) were characterized by intermediate DOC concentrations (4.7–5.4 mg/L), and the remaining 10 lakes were characterized by the highest DOC concentrations (8.3–12.8 mg/L). DOC was positively correlated to elevation and negatively related to temperature (excluding the three "volcanic" lakes). This might reflect the higher inputs of soil DOC in lakes more strongly influenced by inputs from the páramos. The negative relation between DOC and conductivity is consistent with the idea that soils richer in organic matter tend to lead to less mineralized water. Low inputs of soil DOC in the three "volcanic" lakes are possibly related to a low ratio of catchment area to lake surface area, reducing the inputs from soils to the lake. Additionally, the DOC content could be partly modulated by lake size, as indicated by the negative relation between DOC concentration and lake area (Fig. 3). Small lakes might have a greater connectivity and potential exchange of organic carbon with the riparian wetlands and surrounding terrestrial landscape along

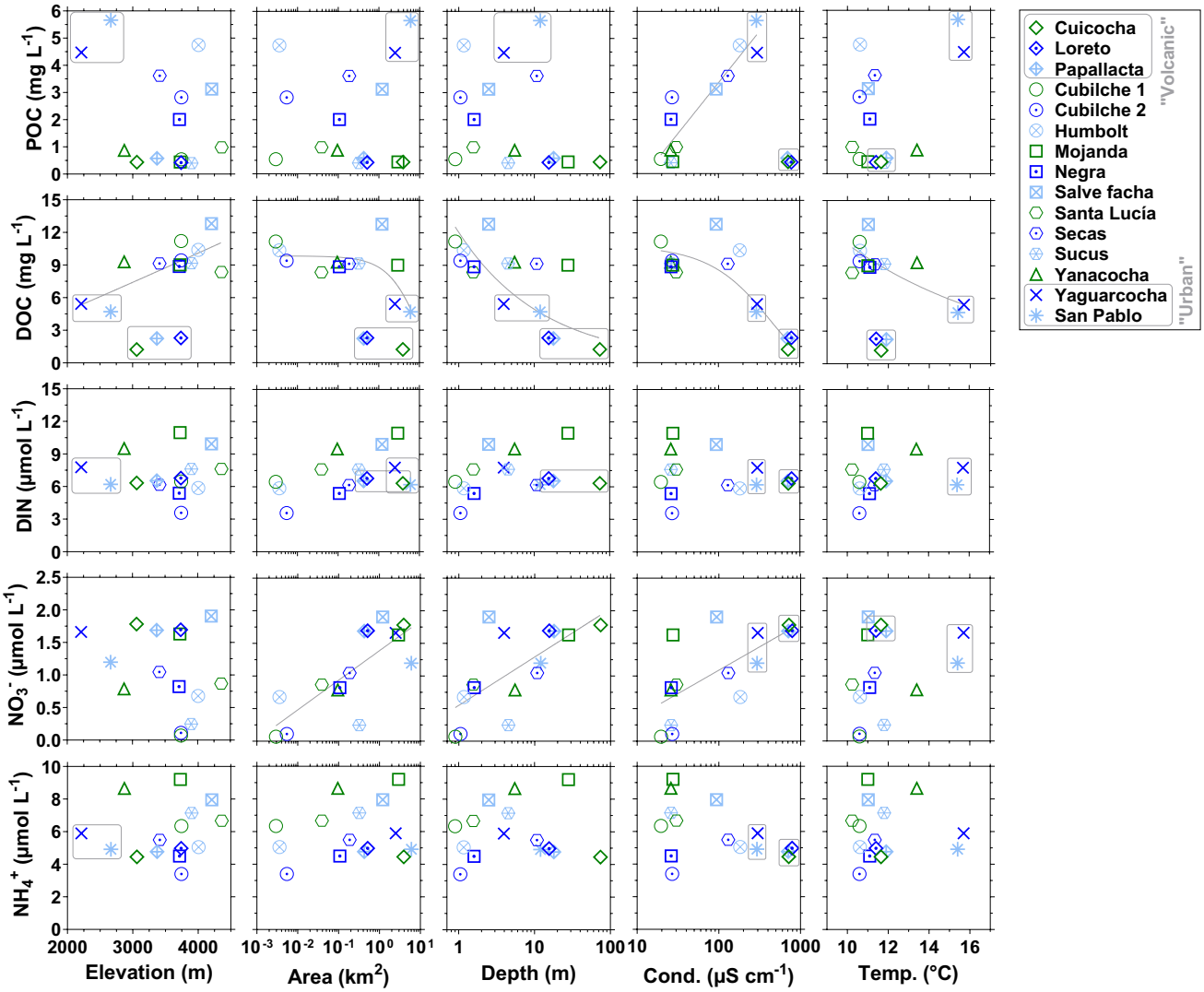

Fig. 3 Particulate (POC in mg/L, relative analytical precision ± 5%) and dissolved (DOC in mg/L, relative analytical precision ± 5%) organic carbon, dissolved inorganic nitrogen (DIN in µmol/L), NO_3^- (µmol/L, analytical precision 0.1 µmol/L) and NH_4^+ (µmol/L, analytical precision 0.02 µmol/L) in surface waters of 15 highland lakes in Northern Ecuador (Fig. 1) versus elevation (m), lake surface area (km^2), lake depth (m), specific conductivity (cond. µS/cm, analytical precision ± 0.1 µS/cm), and water temperature (temp. °C, analytical precision ± 0.1 °C). Solid grey lines show fits to the data (Table S2)

its periphery relative to lake surface area than larger lakes (Staehr et al. 2012). The two above explanations of DOC patterns are compatible as lake size decreases with elevation and the smaller lakes were, thus, located in the páramos with organic carbon rich soils. The POC concentrations ranged between 0.4 and 5.7 mg/L, and the POC data points were less clearly clustered than DOC data points and did not correlate with elevation, lake area, lake depth, or water temperature but did show a relationship with conductivity (Fig. 3). One of the two "urban" lakes (San Pablo) was characterized by the highest POC value (5.7 mg/L), while the three "volcanic" lakes were characterized by some the lowest POC values (0.4–0.6 mg/L). The correlation of POC with conductivity (excluding the three "volcanic" lakes) might possibly reflect a general dilution pattern by meteoric water of solutes and POC. Variations of DIN were modest (3.6–11.0 µmol/L) and DIN did not significantly correlate with elevation, lake area, lake depth, conductivity, and water temperature. DIN was dominated by NH_4^+ (70–98%) that ranged between 3.4 and 9.2 µmol/L. NH_4^+ did not significantly correlate with elevation, lake area, lake depth, conductivity, and water temperature. NO_3^- ranged between 0.1 and 1.9 µmol/L and did not significantly correlate with elevation and temperature but correlated positively to lake area, lake depth, and conductivity. These correlations might possibly reflect a stronger impact in smaller and shallower water bodies of soil–water inputs with a low NO_3^- content related to denitrification in highland soils (Pineda et al. 2021). The NH_4^+ and NO_3^- values we report in Ecuadorian lakes were consistent with those in 51 páramo lakes in the Colombian Andes investigated by Zapata et al. (2021) who reported an average NH_4^+ concentration of 36 µmol/L (range 20–60 µmol/L), and an average NO_3^- concentration of 1.1 µmol/L (range 0.1–12.8 µmol/L).

The pCO_2 values ranged between 208 and 10,069 ppm (Fig. 4). The pCO_2 data points appeared to be grouped into the same three clusters observed for DOC (Fig. 4). The three "volcanic" lakes (Cuicocha, Loreto, and Papallacta) were characterized by higher pCO_2 values (3269–10,069 ppm),

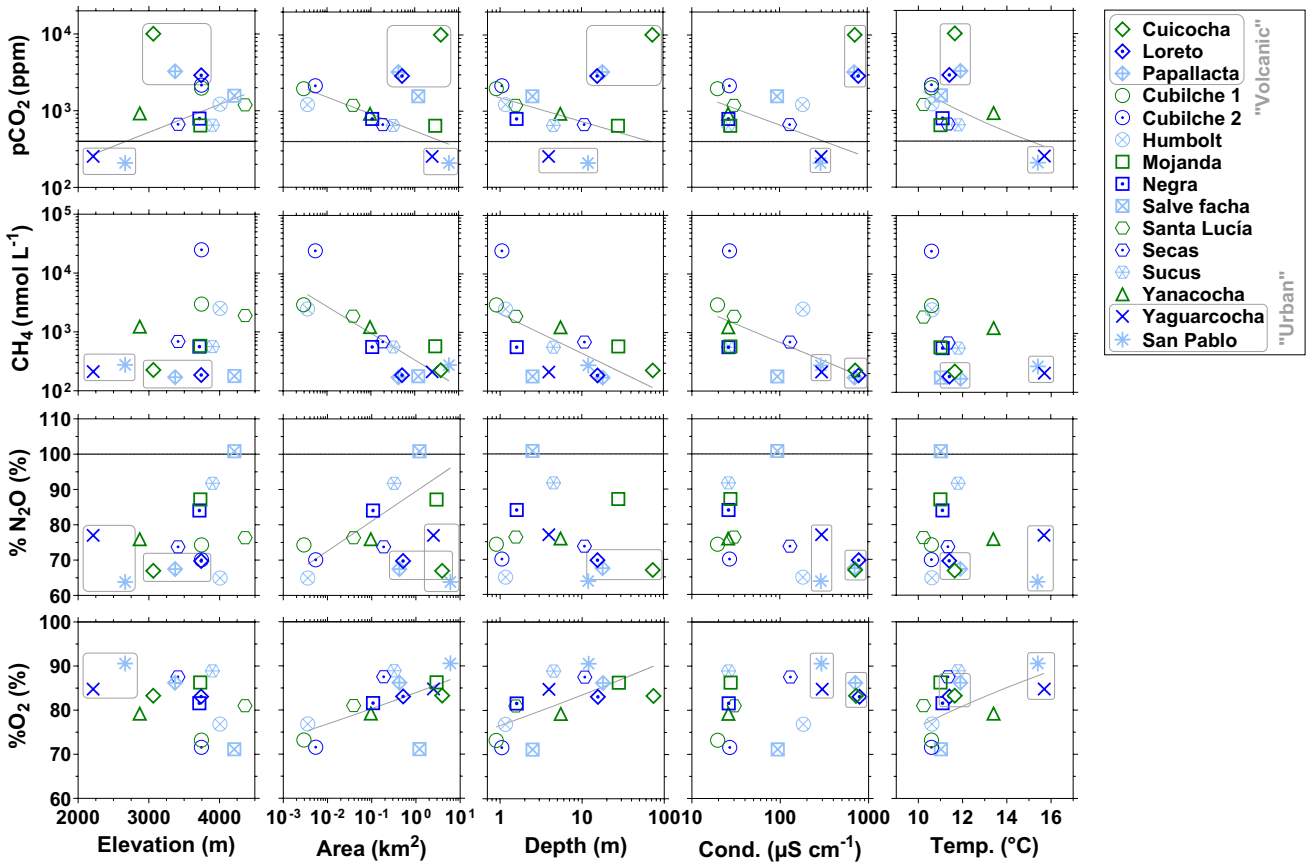

Fig. 4 Partial pressure of CO_2 (pCO_2 in ppm, relative analytical precision ± 5.2%), dissolved CH_4 concentration (nmol/L; relative analytical precision ± 10.9%), N_2O saturation level (%N_2O in %, relative analytical precision ± 5.8%), and O_2 saturation level (%O_2 in %, analytical precision ± 0.1%) in surface waters of 15 highland lakes in Northern Ecuador (Fig. 1) versus elevation (m), lake surface area (km^2), lake depth (m), specific conductivity (cond. µS/cm, analytical precision ± 0.1 µS/cm), and water temperature (Temp. °C analytical precision ± 0.1 °C). Dotted horizontal lines indicate equilibrium of respective gases with the atmosphere and solid grey lines show fits to the data (Table S2)

the two "urban" lakes (San Pablo and Yaguarcocha) by the lowest pCO_2 values (208–254 ppm), and the other páramo lakes by intermediary pCO_2 values (644–2152 ppm). All lakes had pCO_2 values above atmospheric equilibrium (400 ppm) and, thus, acted as sources of CO_2 to the atmosphere, except for the two "urban" lakes that acted as sinks of atmospheric CO_2. The highest pCO_2 values in the three "volcanic" lakes seemed to be in part related to geogenic CO_2 inputs, reflecting the influence of postvolcanic activities, such as emission of volcanic gases and input of hydrothermal water. The δ^{13}C-DIC values in surface waters of the "volcanic" lakes were extremely high (~ 3.5‰) (Fig. S4), and magmatic inputs likely provide the dominant imprint on δ^{13}C-DIC signatures as also reported in Lakes Kivu (~ 1.0‰) and Sonachi (~ 9.0‰) (also a crater lake) (Borges et al. 2012). The δ^{13}C values of volcanic CO_2 in gas bubbles in Ecuadorian crater lakes range between −2% and −6‰ (Inguaggiato et al. 2010; Melián et al. 2021). Consequently, the positive δ^{13}C-DIC values observed in the three "volcanic" lakes also probably reflect the uptake of ^{12}C by primary production and enrichment in ^{13}C in the residual DIC. This effect might be possibly enhanced by long water residence time typical of small crater lakes devoid of outlets. The two "urban" lakes were also characterized by enriched δ^{13}C-DIC signatures, also possibly indicative of uptake of ^{12}C by primary production consistent with the low pCO_2 values (and high POC values). A general increase of δ^{13}C-DIC was observed from $(HCO_3^- + CO_3^{2-})$:DIC = 0.5 (half of the DIC is in the form of CO_2) toward $(HCO_3^- + CO_3^{2-})$:DIC = 1 (all of the DIC is in the form of $HCO_3^- + CO_3^{2-}$). This pattern possibly reflected a gradient of lakes from systems with low rock weathering due to dominance of deep organic soils (low HCO_3^-) and high CO_2 from respiration leading to $(HCO_3^- + CO_3^{2-})$:DIC close to 0.5 with low δ^{13}C-DIC and lakes with higher rock weathering leading to $(HCO_3^- + CO_3^{2-})$:DIC closer to 1 with high δ^{13}C-DIC.

The pCO_2 values in the páramo lakes were positively correlated to elevation and negatively correlated to lake area, lake depth, temperature, and conductivity (excluding the three "volcanic" lakes—Cuicocha, Loreto and Papallacta). This was indicative of higher lacustrine pCO_2 values in páramo lakes bordered by soils with a higher organic carbon content, as shown above for DOC (Fig. 3). Indeed, pCO_2 was positively correlated to DOC, negatively to $\%O_2$ and POC (Fig. 5). This possibly indicated a gradient of inputs of soil water with a low O_2 and conductivity and high DOC and pCO_2 among the páramo lakes that were more important at high elevations owing to soils with a higher organic matter content. Alternatively, the negative relation between pCO_2 and $\%O_2$ could also reflect an internal production of CO_2 within the lakes (and concurrent consumption of O_2) by respiration of allochthonous organic matter, mostly in dissolved form, indirectly leading to a positive relation between pCO_2 and DOC. The implications of the relation between pCO_2 and DOC are discussed in more detail hereafter. Conversely, in lakes with lower inputs of soil DOC (the "urban" lakes

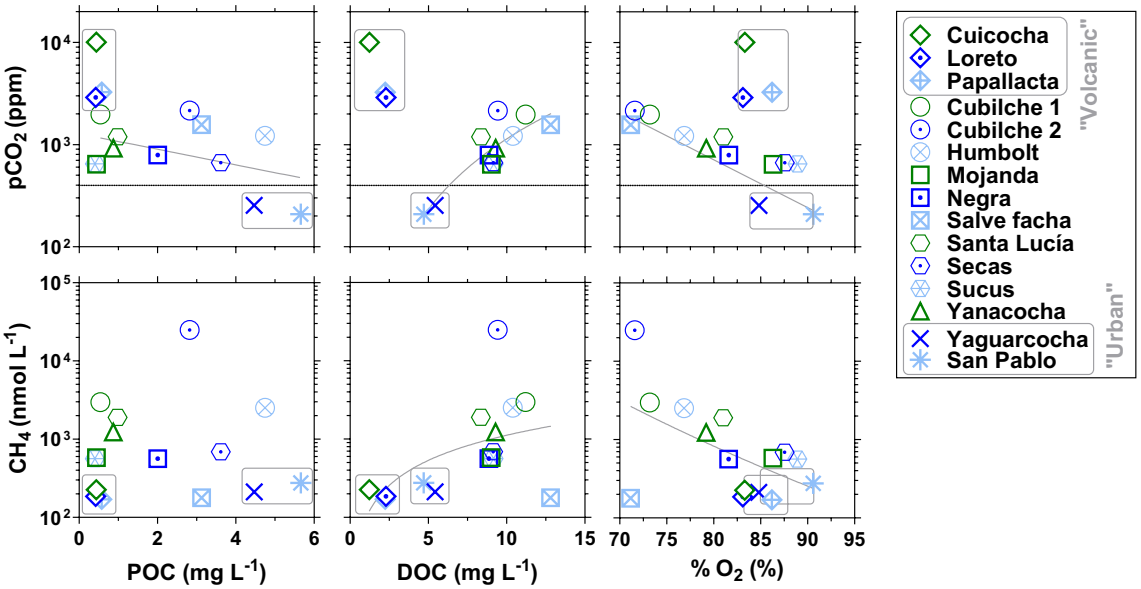

Fig. 5 Partial pressure of CO_2 (pCO_2 in ppm, relative analytical precision ± 5.2%) and dissolved CH_4 concentration (nmol/L, relative analytical precision ± 10.9%) versus particulate (POC in mg/L relative analytical precision ± 5%) and dissolved (DOC in mg/L relative analytical precision ± 5%) organic carbon and O_2 saturation level ($\%O_2$ in %, analytical precision ± 0.1%) in surface waters of 15 highland lakes in Northern Ecuador (Fig. 1). Dotted horizontal lines indicate equilibrium with the atmosphere and solid grey lines show fits to the data (Table S2)

at lower elevation), the lower DOC concentrations might have allowed the development of phytoplankton (lesser light limitation, e.g. Karlsson et al. 2009; Seekell et al. 2015) contributing to the decreasing pattern of pCO_2 with decreasing DOC and increasing POC. Additionally, the lakes at higher elevation tended to be shallower and smaller (Fig. 2). As mentioned above to explain the pattern of DOC and lake size, smaller lakes should have a greater connectivity and potential exchange of CO_2 from soils along their periphery relative to lake surface area (Staehr et al. 2012). Also, there is a stronger fetch limitation of k in smaller lakes (Wanninkhof 1992) that can possibly contribute to the accumulation of CO_2 in lake surface water of smaller lakes, while higher k in larger lakes can promote degassing and bring CO_2 levels closer to atmospheric equilibrium. These processes combined possibly contributed to the explanation of the negative relation between pCO_2 with lake surface area as well as with lake depth (Fig. 4). Since the CO_2 dynamics were related to organic matter degradation (in soils or in lake), $\%O_2$ correlated to pCO_2 (Fig. 5) and $\%O_2$ patterns mirrored those of pCO_2: $\%O_2$ was positively related to lake area, lake depth, and water temperature but was not significantly correlated to conductivity and elevation (Fig. 4).

Dissolved CH_4 concentrations ranged between 170 and 24,908 nmol/L in the sampled lakes (Fig. 4). Dissolved CH_4 concentrations were not significantly correlated to elevation, water temperature, and POC but were negatively correlated to lake area, lake depth, conductivity, DOC and $\%O_2$ (Figs. 4, 5). The patterns of CH_4 paralleled those of pCO_2. The smaller lakes bordered by soils with a higher organic carbon content were likely characterized by a higher CH_4 production in lake sediments or in surrounding soils. Additionally, smaller lakes were generally shallower, also potentially affecting the relative removal of CH_4 by bacterial oxidation compared with the sedimentary input of CH_4, probably resulting in higher CH_4 dissolved concentrations in shallower lakes (Borges et al. 2011; 2022).

$\%N_2O$ ranged between 63.8% and 100.8%. All the sampled lakes were sinks of atmospheric N_2O, except Salve Fecha, which was close to saturation (100.8%). This possibly implies a removal of N_2O by denitrification due to the complete reduction of N_2O to N_2. $\%N_2O$ did not significantly correlate to elevation, lake depth, conductivity, and temperature but correlated to lake area (Fig. 4). NO_3^- also correlated with lake area (Fig. 3). Similar patterns of $\%N_2O$ and NO_3^- as a function of lake area might possibly reflect a stronger impact in smaller water bodies of soil–water inputs with low content in N_2O and NO_3^- related to denitrification in highland páramo soils (Pineda et al. 2021). Yet, paradoxically, $\%N_2O$ did not significantly correlate with NO_3^- but correlated with NH_4^+ (and thus also with DIN) (Fig. 6), although NH_4^+

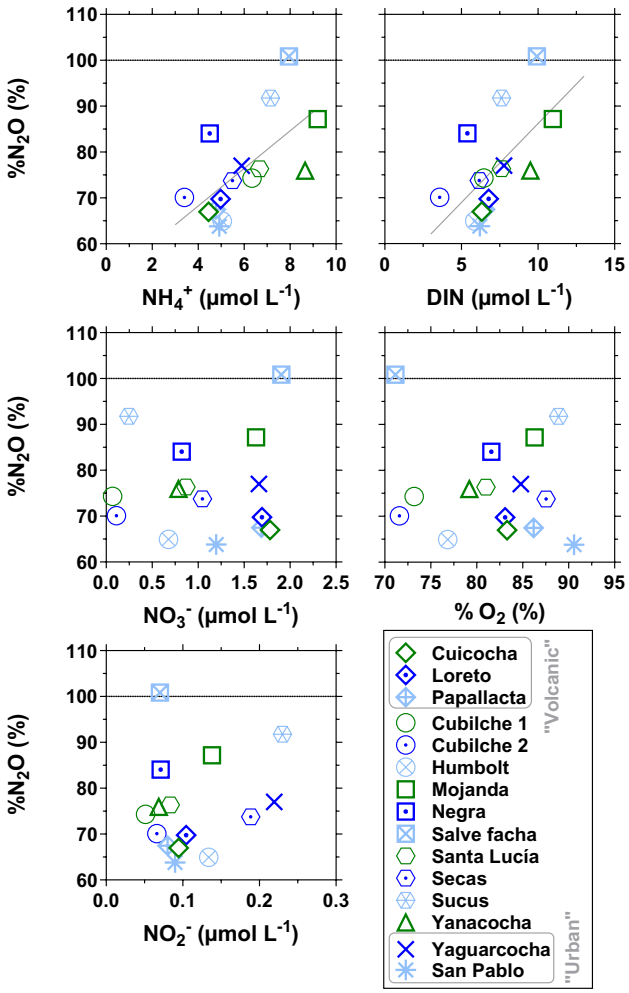

Fig. 6 N_2O saturation level ($\%N_2O$ in %, relative analytical precision ± 5.8%) versus NH_4^+ (µmol/L, analytical precision ± 0.02 µmol/L), dissolved inorganic nitrogen (DIN in µmol/L), NO_3^- (µmol/L, analytical precision ± 0.1 µmol/L), NO_2^- (µmol/L, analytical precision ± 0.02 µmol/L) and O_2 saturation level ($\%O_2$ in %, analytical precision ± 0.1%) in surface waters of 15 highland lakes in Northern Ecuador (Fig. 1). Dotted horizontal lines indicate equilibrium with the atmosphere and solid grey lines show fits to the data (Table S2)

did not correlate with lake area (Fig. 3). $\%N_2O$ did not also significantly correlate to NO_2^- and $\%O_2$. The general lack of correlation of $\%N_2O$ with other variables might possibly reflect that there was a low contribution of internal cycling of N_2O within the lakes and that the N_2O levels in lakes were primarily controlled by the inputs of soil–water in a low N_2O level related to soil denitrification. Additionally, N_2O was driven closer to equilibrium with the atmosphere in larger lakes where k increases with fetch (Wanninkhof 1992). Combined, these two processes might possibly explain the relation between $\%N_2O$ and lake surface area.

Comparison with floodplain lakes in central Amazon

The sampled páramo lakes were generally smaller (1.1 ± 1.9 km^2, average ± standard deviation) with higher DOC concentration (9.0 ± 2.2 mg/L) than the lowland floodplain lakes compiled from literature (183 ± 311 km^2; 5.3 ± 1.1 mg/L) (Fig. 7). Yet, the pCO_2 values in lowland floodplain lakes were higher (3115 ± 1605 ppm) than in the páramo lakes (1037 ± 615 ppm), even for overlapping values of depth, lake surface area, and DOC concentrations (Fig. 7). This pattern probably resulted from inputs of fluvial CO_2 in the floodplain lakes that led to higher pCO_2 values than in the páramo lakes. Bidirectional flows between rivers and floodplains determine the ecological functioning and biogeochemical fluxes of Amazonian floodplain lakes (Junk et al. 1989), including CO_2 dynamics (Abril et al. 2014; Amaral et al. 2018). The pattern of lower pCO_2 values in mountainous lakes compared with lowland lakes generally agrees with other studies of CO_2 dynamics in mountainous lakes at higher latitude, such as in the Alps (Pighini et al. 2018), Rocky Mountains (McCrackin and Elser 2011; Crawford et al. 2015), Sierra Nevada (Cohen and Melack 2020), and the Tibetan Plateau (Yan et al. 2018, 2023; Wang et al. 2022).

The pCO_2 values were positively correlated to water temperature across the data set merging highland and lowland lakes (Fig. S5). This correlation could be spurious, reflecting the altitudinal gradient in pCO_2 and does not necessarily reflect a temperature dependence of inputs of CO_2 to the lake, such as aquatic respiration within the lake or inputs of CO_2 from the soils of the watershed related to soil respiration. Regarding soil respiration, it is difficult to disentangle

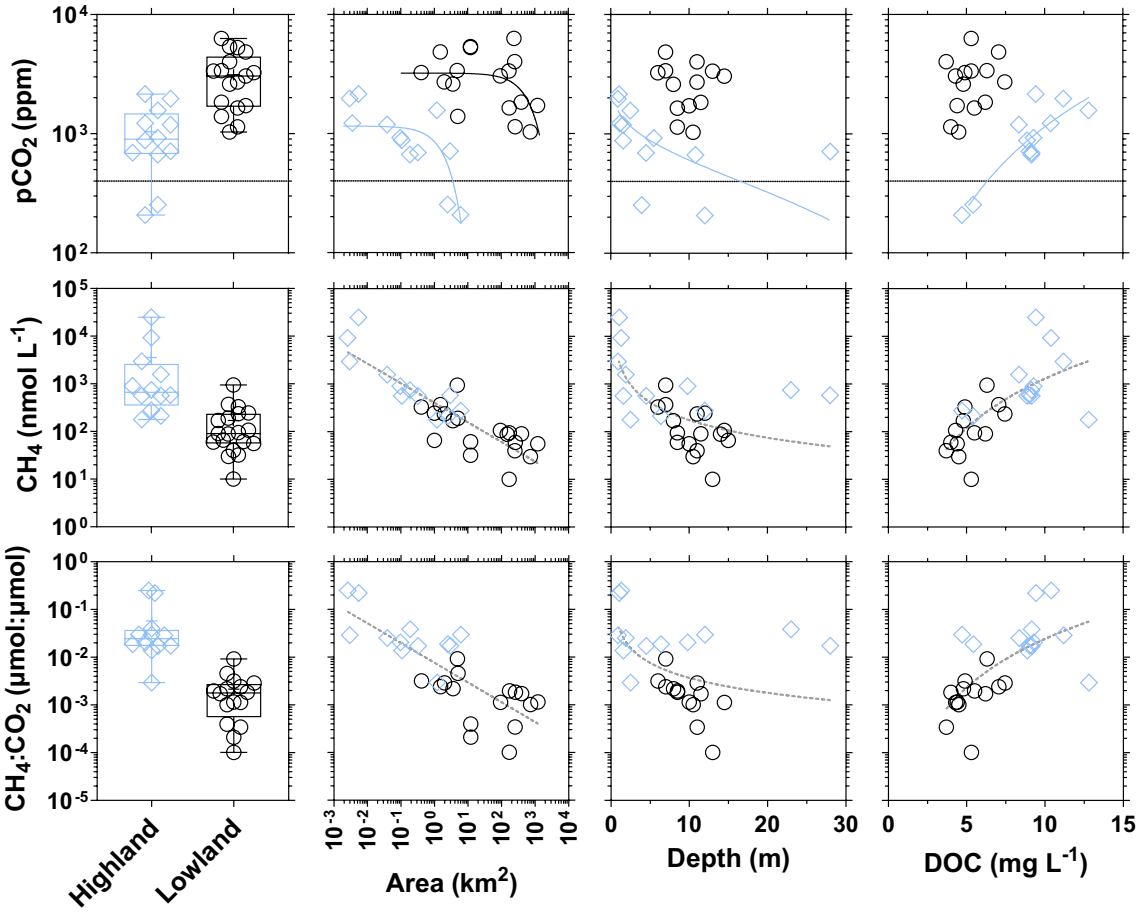

Fig. 7 Partial pressure of CO_2 (pCO_2 in ppm, relative analytical precision ± 5.2%), dissolved CH_4 concentration (nmol/L, relative analytical precision ± 10.9%), and CH_4:CO_2 ratio (µmol:µmol) versus lake surface area (km^2), lake depth (m), and dissolved organic carbon (DOC in mg/L, relative analytical precision ± 5%) in the sampled highland lakes in Northern Ecuador (excluding lakes Cuicocha, Loreto, and Papallacta influenced by volcanic inputs) and in lowland floodplain lakes of the Amazon basin gathered from literature (Abril et al. 2013; Albéric et al. 2018; Amaral et al. 2020; Barbosa et al. 2016; Mitchell et al. 2018). For pCO_2, only data directly measured by equilibration were compiled, data computed from pH and total alkalinity were excluded as they can be prone to large errors (Abril et al. 2015). Dotted horizontal lines indicate equilibrium with the atmosphere and solid lines show fits to the data (Table S2) (blue solid lines are highland lakes; black solid lines are lowland lakes; grey dotted lines are high- and lowland lakes)

the effects of variations of soil properties and of temperature across altitudinal gradients, since both vary along the altitudinal gradient (Badraghi et al. 2021). Pineda et al. (2021) reported a data set of soil–air emissions of CO_2 in Ecuadorian Andes along an altitudinal gradient (3000–400 m). Soil–air emissions of CO_2 were higher at 3000 m due to higher organic carbon content than at 400 m despite lower temperatures (~ 12 °C versus ~ 22 °C, respectively). Since soil–air CO_2 emissions are a function of soil respiration, the potential CO_2 inputs from soils to lakes could in fact be stronger at higher altitudes than lower altitudes; however, lower CO_2 concentrations were observed in the higher altitude lakes compared with the lakes in the Central Amazon. This would suggest an additional external CO_2 input in lowland lakes compared with highland lakes.

Respiration in lake sediments scales with temperature (Cardoso et al. 2014); however, respiration in the water column of lakes seems more strongly dependent on organic carbon availability than on temperature (Pace and Prairie 2005). This is in line with a lack of relation between aquatic respiration and temperature in rivers in tropical settings (for a temperature gradient between ~ 12 °C and ~ 27 °C) (Marzolf and Ardón 2021), as well as across climate zones (Bernhardt et al. 2022). So, other factors than temperature, such as organic matter availability, seem to govern the variability of aquatic respiration in lakes and rivers.

We hypothesize that the positive relation between pCO_2 and temperature did not result primarily from the temperature dependence of aquatic respiration within the lakes. If the CO_2 was mainly coming from soils, higher CO_2 would have been expected in higher altitude lakes due to the higher soil respiration (Pineda et al. 2021) and, generally, lower lake size of sampled lakes that should have led to a stronger influence from soil inputs (Staehr et al. 2012). Hence, the hypothesis of riverine inputs of CO_2 from the Amazon River in driving higher pCO_2 values in lowland lakes might possibly be more appropriate and in line with the importance of bidirectional flows between rivers and floodplains for the carbon fluxes of Amazonian floodplain lakes (Junk et al. 1989; Abril et al. 2014; Amaral et al. 2018).

The CH_4 values in the sampled highland lakes were higher (3564 ± 7186 nmol/L) than in the floodplain lakes in the Central Amazon basin (170 ± 215 nmol/L) compiled from literature (Fig. 7). Yet, CH_4 concentration was correlated with depth, lake surface area, and DOC across the full data set including both highland and lowland lakes. A tighter relation between CH_4 and lake morphology (depth and surface area) would suggest a dominant effect of lake size on the internal production and external inputs from soils of CH_4 despite different settings across the elevational gradient in the whole Amazon basin. Such an effect seems to override the difference in water temperature between highland (12.4 ± 1.9 °C) and lowland lakes (30.7 ± 1.4 °C), despite the fact that methanogenesis shows a strong temperature dependence (Yvon-Durocher et al. 2014). The CH_4 values were negatively correlated to water temperature across the data set merging highland and lowland lakes (Fig. S5). Such a correlation seemed spurious since CH_4 fluxes would be expected to be positively related to temperature (Yvon-Durocher et al. 2014). In a recent meta-analysis at global scale, no relation was found between temperature and CH_4 emissions from lakes (Deemer and Holgerson 2021) and rivers (Rocher-Ros et al. 2023).

The consistency across the data set of the relation between CH_4 and surface area differed from pCO_2, for which there were distinct relationships with surface area for highlands and lowlands, possibly reflecting local drivers specific to lowlands compared with highlands, in particular the connectivity with the Amazon river channel in the floodplain lakes. Consequently, unlike CH_4, a simple "unifying" correlation between pCO_2 and other variables (DOC, lake size) did not emerge for both highland and lowland lakes from our data set. Since CH_4 was higher and CO_2 lower in highland lakes compared with lowland lakes, the CH_4:CO_2 ratio was markedly higher and also correlated with lake surface area, depth and DOC (Fig. 7).

The pCO_2 was not correlated with DOC across the whole basin suggesting that pCO_2-DOC relationship was regionally specific, as also suggested in boreal landscapes (Roehm et al. 2009; Lapierre and del Giorgio 2012). This would suggest that the relation of pCO_2 and DOC results from multiple processes and do not provide consistent and reproducible patterns across large regions as noted in boreal landscapes. This is possibly related to regional patterns in DOC composition and/or in landscape morphology and lake position in the landscape that dictate the amount and relative proportions of DOC and CO_2 exports from soils to lakes (Roehm et al. 2009; Lapierre and del Giorgio 2012). This is also in line with a recent analysis of pCO_2 in African lakes showing diverging pCO_2-DOC relations in different type of lakes, in particular in humic and nonhumic lakes (Borges et al. 2022). In our particular case, the difference between highland and lowland pCO_2-DOC patterns is most likely related to the strong influence of riverine inputs in lowland floodplain lakes. It is unclear if the correlation between CH_4 and DOC is spurious or reflects a causal relation. This relation could be spurious because shallower lakes tend to have higher CH_4 concentrations due to the lower effect of the removal of CH_4 by methane oxidation and stronger effect of CH_4 inputs from sediments or soils (Borges et al. 2011; Holgerson and Raymond 2016). Shallower lakes tended to be smaller in our data set, and smaller water bodies tend to have higher DOC concentrations because small lakes have a greater connectivity and potential exchange of organic carbon with the riparian wetlands and surrounding terrestrial

landscape along its periphery relative to lake surface area than larger lakes (Staehr et al. 2012).

Emissions of CO_2 and CH_4 from lakes and streams of the Amazon basin

We use relationships as a function of lake surface area (Fig. 7) to scale pCO_2 and dissolved CH_4 concentration to all the lakes in the Amazon basin ($n = 12{,}549$) given by the HydroLAKES data set (Messager et al. 2016). The relationships combined our data in Ecuadorian highland lakes and data compiled from the literature for lowland lakes in the Central Amazon, totaling 34 lakes for CH_4 and 29 lakes for CO_2. For CH_4, there was a robust relation with lake surface area across the whole Amazon basin (Fig. 7). For consistency, we also used a relation as a function of lake surface area to scale pCO_2, but two separate relations were needed for highland and lowland lakes. Such an approach is applicable because the distribution of lake numbers and surface areas given by HydroLAKES follows a bimodal distribution, with the majority located in lowlands (elevation < 500 m) followed by highlands (elevation > 2500 m) with very few lakes located at elevations between 500 and 2500 m (Fig. S6). We upscaled CH_4 diffusive fluxes using surface area as a predictor (Fig. 7), because the range of depth variations was restricted in the highland (average 8 ± 9 m range 1–28 m) and in the lowland (average 10 ± 3 m range 6–15 m) lakes, in line with previous studies in small and shallow water bodies (Holgerson and Raymond 2016). The ebullitive FCH_4 was not measured in the sampled Ecuadorian lakes, and we extracted for lakes of the Amazon basin the values modeled by Borges et al. (2022) in tropical lakes globally. This model relies on a compilation of ebullitive FCH_4 data in tropical lakes extrapolated to the littoral zone (depth < 10 m), for which the surface area was derived from morphometric relations based on maximum depth (Håkan et al. 2007) applied to HydroLAKES (Messager et al. 2016). The CO_2 and CH_4 diffusive fluxes in the streams and rivers of the Amazon basin were reported by Chiriboga and Borges (2023) and relied on statistical modelling of CO_2 and CH_4 concentrations applied to RiverAtlas (Linke et al. 2019). Data of ebullitive FCH_4 have only been reported in nine large rivers of the Amazon basin (Sawakuchi et al. 2014). We estimated ebullitive FCH_4 for the rivers and streams assuming they equaled the values of diffusive FCH_4, as reported by a global compilation ($n = 93$) by Rocher-Ros et al. (2023).

The diffusive CH_4 emission (0.0007 ± 0.0003 TgC/yr) from highland lakes (elevation > 500 m) was 18 times lower than from lowland lakes (elevation < 500 m) (0.0130 ± 0.006 TgC/yr) (Table 2). This was due to lakes in the lowlands being 11 times more numerous (12,549 versus 1116) and covering a surface area 23 times larger (22,282 versus 952 km^2) than in the highlands (Fig. S6, Table 2). The average areal diffusive FCH_4 (per m^2) in highland lakes (0.75 ± 0.36 $gC/m^2/yr$) was close to the FCH_4 in lowland lakes (0.58 ± 0.28 $gC/m^2/yr$) owing to similar dissolved CH_4 concentrations (265 nmol/L versus 179 nmol/L) but marginally higher k values (3.5 ± 0.5 cm/h versus 2.5 ± 0.3 cm/h). The average dissolved CH_4 concentration was similar in highland lakes because of equivalent average surface areas (0.85 ± 5.54 km^2) in highland and lowland (1.78 ± 15.54 km^2) lakes. The k values were on average marginally higher in highland lakes because of higher average wind speed (3.0 ± 0.6 m /s) than lowland lakes (1.4 ± 0.6 m /s) (Table 2). The ebullitive FCH_4 in lakes (0.41 ± 0.21 TgC/yr) modeled by Borges et al. (2022) was 31 times higher than the diffusive FCH_4 (0.014 ± 0.006 TgC/yr), as generally reported in lakes (Deemer and Holgerson 2021; Borges et al. 2022; Johnson et al. 2022). The total FCH_4 (ebullitive and diffusive, 0.42 ± 0.21 TgC/yr) from lakes in the Amazon basin we computed was within the range (0.10–0.53 TgC/yr) modeled with one-dimensional process-based lake biogeochemical model (Guo et al. 2020) calibrated with data from lakes Calado and Janauacá (respectively) (Melack et al. 2022), and similar to the estimate of ~ 0.5 TgC/yr reported by Malhi et al. (2021) based on the extrapolation of the average fluxes from a single lake (Lake Janauacá, Barbosa et al. 2020).

The areal diffusive FCH_4 was higher in rivers than lakes in both lowlands (6.8 ± 2.1 versus 0.6 ± 0.3 $gC/m^2/yr$) and highlands (12.9 ± 2.9 versus 0.8 ± 0.4 $gC/m^2/yr$) due to much higher k values (16–149 versus 3–4 cm/h), while average CH_4 was higher in rivers (427 nmol/L) than lakes (179 nmol/L) in lowlands, but the opposite was observed in highlands (157 versus 265 nmol/L). Integrated diffusive FCH_4 was higher in rivers than lakes in both lowlands (0.27 ± 0.08 versus 0.01 ± 0.01 TgC/yr) and highlands (0.03 ± 0.01 versus 0.001 ± 0.001 TgC/yr) because the surface area covered by rivers was higher than lakes in lowlands (40,375 versus 22,282 km^2) and highlands (2338 versus 952 km^2), in addition to higher areal diffusive FCH_4 values. Ebullitive FCH_4 was equivalent in rivers and lakes in lowlands (0.27 ± 0.08 versus 0.41 ± 0.21 TgC/yr) and highlands (0.03 ± 0.01 versus 0.01 ± 0.01 TgC/yr). The total (diffusive and ebullitive) FCH_4 from rivers (0.61 ± 0.12 TgC/yr) was close to the total (diffusive and ebullitive) FCH_4 from lakes (0.43 ± 0.21 TgC/yr), at the scale of the whole Amazon basin. The total (diffusive and ebullitive) FCH_4 from lakes alone (0.43 ± 0.21 TgC/yr) and from lakes plus rivers (1.04 ± 0.24 TgC/yr) only represented ~ 1.4% and ~ 3.3%, respectively, of total CH_4 emissions from all compartments of the Amazon basin ranging between 30 and 34 TgC/yr derived from top-down estimates based on aircraft or satellite data (Wilson et al. 2016, 2021; Pangala et al. 2017), which are mainly attributable to wetlands (Basso et al. 2021).

Table 2 Emissions to the atmosphere of CO_2 (FCO_2) and CH_4 (FCH_4) from the lakes and rivers of the Amazon basin

	Elevation	
	< 500 m	> 500 m
Lakes		
Diffusive FCH_4 (TgC/yr)	0.0130 ± 0.006	0.0007 ± 0.0003
Diffusive FCH_4 (gC/m^2/yr)	0.58 ± 0.28	0.75 ± 0.36
Ebullitive FCH_4 (TgC/yr)	0.41 ± 0.21	0.009 ± 0.005
Ebullitive FCH_4 (gC/m^2/yr) *	18.5 ± 9.2*	9.5 ± 4.7*
Surface area weighted average CH_4 (nmol/L)	179	265
Diffusive FCO_2 (TgC/yr)	5.7 ± 1.9	0.022 ± 0.015
Diffusive FCO_2 (gC/m^2/yr)	255 ± 86	23 ± 16
Surface area weighted average pCO_2 (ppm)	2909	530
Wind speed (m /s)	1.4 ± 0.6	3.0 ± 0.6
k_{600} (cm/h)	2.5 ± 0.3	3.5 ± 0.5
Total lake surface area (km^2)	22,282	952
Number of lakes	12,549	1116
Average lake surface area (km^2)	1.78 ± 15.54	0.85 ± 5.54
Rivers		
Diffusive FCH_4 (TgC/yr)	0.273 ± 0.084	0.030 ± 0.007
Diffusive FCH_4 (gC/m^2/yr)	6.77 ± 2.08	12.93 ± 2.88
Ebullitive FCH_4 (TgC/yr) **	*0.273***	*0.030***
Ebullitive FCH_4 (gC/m^2/yr) **	*6.77***	*12.93***
Average CH_4 (nmol/L)	427	157
Diffusive FCO_2 (TgC/yr)	58.9 ± 4.1	5.5 ± 1.0
Diffusive FCO_2 (gC/m^2/yr)	1459 ± 103	2364 ± 418
Average pCO_2 (ppm)	2702	1033
k_{600} (cm/h)	15.8 ± 0.4	148.8 ± 3.2
Total stream surface area (km^2)	40,375	2338

The diffusive FCO_2 and FCH_4 in lakes was modeled from relations of CO_2 and CH_4 dissolved concentration as a function of lake surface area based on our data in Ecuadorian highland lakes and data from literature for lowland floodplain lakes (Fig. 7), using the HydroLAKES spatial data set (Messager et al. 2016) and the gas transfer velocity (k_{600}) derived from a parameterization as a function of wind speed (Cole and Caraco 2018) and wind speed from the WorldClime spatial data set (Fick and Hijmans 2017). The ebullitive FCH_4 in lakes was modeled by Borges et al. (2022) from a compilation of data in tropical lakes extrapolated to the littoral zone (depth < 10 m) for which the surface area was derived from morphometric relations based on maximum depth (Håkan et al. 2007) applied to HydroLAKES (Messager et al. 2016). The diffusive FCO_2 and FCH_4 in rivers was modeled by Chiriboga and Borges (2023) from of CO_2 and CH_4 dissolved concentration as a function of catchment slope, k_{600} derived from a parameterization as a function of stream slope and flow (Raymond et al. 2012) and the RiverATLAS spatial data set (Linke et al. 2019). The ebullitive FCH_4 in rivers was assumed identical to the diffusive FCH_4 as reported by a global compilation ($n = 93$) by Rocher-Ros et al. (2023)

*The areal flux was rescaled for the total lake surface rather than the surface area of the littoral zone (depth < 10 m)

**For rivers, ebullitive FCH_4 was assumed equal to diffusive FCH_4 based on Rocher-Ros et al. (2022)

The CO_2 emission (0.022 ± 0.015 TgC/yr) from highland lakes was 257 times lower than from lowland lakes (5.7 ± 1.9 TgC/yr) (Table 2). The average areal FCO_2 from lakes was also 11 times lower in highlands (23 ± 16 gC/m^2/yr) than in lowlands (255 ± 86 gC/m^2/yr) owing to the lower pCO_2 values (530 ppm versus 2909 ppm) despite higher k values (3.5 ± 0.5 cm/h versus 2.5 ± 0.3 cm/h). The CO_2 emission from lakes from the Amazon basin we computed (5.7 ± 1.9 TgC/yr) was 4.1 times lower than the one reported by Raymond et al. (2013) (23.3 TgC/yr). This difference is related to a lower lake surface area (23,234 versus 51,629 km^2) and a lower areal FCO_2 (245 versus 451 gC/m^2/yr) that is due to lower k values (2.5 versus 5.7 cm/h). Our averaged pCO_2 value was in fact marginally higher than the one used by Raymond et al. (2013) (2811 versus 1906 ppm). The lake surface area used by Raymond et al. (2013) was derived from Downing et al. (2006), which includes lakes with a surface area down to 0.001 km^2, while HydroLAKES only

reports lakes with a surface area ≥ 0.1 km^2. The number of lakes with a surface area < 0.1 km^2 reported by Downing et al. (2006) was computed assuming a Pareto distribution which has been questioned on empirical (McDonald et al. 2012) and theoretical (Seekell and Pace 2011) grounds. The HydroLAKES data set has recently been recommended and applied in global scaling of lacustrine GHG emissions (Johnson et al. 2022; Lauerwald et al. 2023). Raymond et al. (2013) used a constant *k* value for several lake size classes calculated from the compilation of *k* values derived from tracer experiments in temperate or boreal systems. We computed the *k* values for each lake from local wind speed derived from WorldClim (Fick and Hijmans 2017) using the *k*-wind parameterization of Cole and Caraco (2018). Wind speed is zonally variable as a function of latitude, and tropical landmasses show distinctly lower values than higher latitude areas, which explained the difference in average *k* for lakes in the Amazon basin we computed and those used by Raymond et al. (2013). Raymond et al. (2013) used an average pCO_2 of 1906 ppm for all tropical lakes based on data set of Sobek et al. (2005) that compiles mostly pCO_2 data computed from pH and TA that are usually overestimated (Abril et al. 2015). The average pCO_2 value proposed by Raymond et al. (2013) for tropical lakes (1906 ppm) was higher than the value we scaled for highland lakes (on average 530 ppm) but lower for lowland lakes (on average 2909 ppm).

The relative contribution of ebullitive and diffusive FCH_4 to total carbon emissions ($CO_2 + CH_4$) was 31% in highland lakes and 7% in lowland lakes (Table 2). The relative contribution of FCH_4 to total carbon emissions ($CO_2 + CH_4$) for the whole Amazon basin (both high- and lowlands) was low in lakes (7%) and rivers (1%).

Conclusions

Global estimates of CO_2, CH_4, and N_2O emissions from lakes and rivers are uncertain because available data sets do not capture the inherent large variability and are insufficient to derive robust statistical functions to scale fluxes with confidence, despite the recent emergence of detailed spatial data sets of location and surface area for rivers (Allen and Pavelsky 2018; Linke et al. 2019) and lakes (Messager et al. 2016) that can be used to scale fluxes. Tropical lakes are undersampled with regards to GHG emissions compared with higher latitude systems, and this is particularly true for mountainous lakes. The CH_4 and pCO_2 values we report in mountainous lakes of the Ecuadorian Andes were very different from those reported in literature for the floodplain lakes of Central Amazon. This seemed to have resulted from smaller size of highland lakes that were surrounded by the páramo organic matter rich soils, which might have possibly led to higher CH_4 levels in highland lakes. The higher pCO_2 values in lowland floodplain lakes probably resulted from inputs of CO_2 from the Amazon River, although we do not exclude other processes such as a higher respiration, in particular in lake sediments, related to higher temperatures.

We modeled the CH_4 and CO_2 emissions from lakes at the scale of the whole basin, using simple statistical relations based on lake surface area. Such a relation with surface area is not fortuitous but is based on well-established links between lake size and external subsidies of carbon from the surrounding landscape (Staehr et al. 2012). Given the restricted range of depth variations in the data set, surface area seemed to be a better predictor than depth to scale the CO_2 and CH_4 data. The resulting estimated CH_4 and CO_2 emissions from lakes had an inherent uncertainty, which was quantified, but should represent an improvement compared with the previous estimate of CH_4 and CO_2 emissions from lakes in the Amazon basin that relied on the extrapolation of the value from a single lake for CH_4 (Malhi et al. 2021) or on the extrapolation of an average value of pCO_2 from tropical lakes in general (Raymond et al. 2012). The uncertainty on the estimated CH_4 and CO_2 emissions from lakes resulted in part from the "one station in the center" snapshot survey approach, although frequently used to investigate broad geographical gradients as a function, for instance, of climate or catchment land cover (Juutinen et al. 2009; Finlay et al. 2010; Lapierre and del Giorgio 2012; Kortelainen et al. 2020; Casas-Ruiz et al. 2021; Rodríguez-Cardona et al. 2023). Additionally, the ebullitive CH_4 emissions were not measured in the Ecuadorian sampled lakes but derived from a statistical model for tropical lakes (Borges et al. 2022). The uncertainty on the estimation of CH_4 and CO_2 emissions from lakes of the Amazon basin could be improved in future by increasing the number of sampled lakes and better accounting for within lake spatial and temporal variability by increasing the number of samples horizontally and in time. The uncertainty on the estimation of CH_4 emissions from lakes of the Amazon basin could be further improved by additional direct measurements of ebullitive CH_4 emissions.

The integrated basin-wide diffusive CO_2 emissions from lakes were much lower than those from the river network. The integrated basin-wide diffusive and ebullitive lake CH_4 emissions were roughly equivalent to those from the river network. The total diffusive and ebullitive CH_4 emissions from lakes and rivers corresponded to a very small fraction (< 2%) of the total CH_4 emissions from all compartments of the Amazon basin, derived from top-down estimates, which are mainly attributable to wetlands.

Supplementary Information The online version contains supplementary material available at https://doi.org/10.1007/s00027-023-01039-6.

Acknowledgements We thank Yannick Stroobandt for analytical assistance with stable isotope and POC and DOC concentration measurements, Gwenaël Abril for providing CH_4 data in Central Amazonian

lakes, and the editor (David Janssen) and two anonymous reviewers for constructive and helpful comments. This research was funded by the *Académie de recherche et d'enseignement supérieur* (ARES). A.V.B. is a research director at the *Fonds National de la Recherche Scientifique*.

Author contributions A.V.B. designed the research and analyzed the data. G.C. collected the samples. G.C. measured the GHGs, TA, and nutrients, and S.B. measured DOC and POC concentrations, H_2O, DIC isotopes, and major elements. A.V.B. drafted the manuscript, with contributions from G.C. and S.B.

Data availability The dataset generated during the current study is publically available from https://doi.org/https://doi.org/10.5281/zenodo.7867344.

Declarations

Conflict of interest The authors declare that they have no conflict of interest.

References

Abril G, Commarieu M-V, Guérin F (2007) Enhanced methane oxidation in an estuarine turbidity maximum. Limnol Oceanogr 52:470–475. https://doi.org/10.4319/lo.2007.52.1.0470

Abril G, Martinez J-M, Artigas LF, Moreira-Turcq P, Benedetti MF, Vidal L, Meziane T, Kim J-H, Bernardes MC, Savoye N, Deborde J, Albéric P, Souza MFL, Souza EL, Roland F (2014) Amazon river carbon dioxide outgassing fuelled by wetlands. Nature 505:395–398. https://doi.org/10.1038/nature12797

Abril G, Bouillon S, Darchambeau F, Teodoru CR, Marwick TR, Tamooh F, Omengo FO, Geeraert N, Deirmendjian L, Polsenaere P, Borges AV (2015) Technical note: Large overestimation of pCO_2 calculated from pH and alkalinity in acidic, organic-rich freshwaters. Biogeosciences 12:67–78. https://doi.org/10.5194/bg-12-67-2015

Albéric P, Pérez MAP, Moreira-Turcq P, Benedetti MF, Bouillon S, Abril G (2018) Variation of the isotopic composition of dissolved organic carbon during the runoff cycle in the Amazon River and the floodplains, C.R. Geoscience 350:65–75. https://doi.org/10.1016/j.crte.2017.11.001

Allen GH, Pavelsky TM (2018) Global extent of rivers and streams. Science 361:585–588. https://doi.org/10.1126/science.aat0636

Altenau EH, Pavelsky TM, Durand MT, Yang X, Frasson RPDM, Bendezu L (2021) The surface water and ocean topography (SWOT) mission river database (SWORD): a global river network for satellite data products. Water Resour Res 57:e2021WR030054. https://doi.org/10.1029/2021WR030054

Amaral JHF, Borges AV, Melack JM, Sarmento H, Barbosa PM, Kasper D, Melo ML, de Fex Wolf D, da Silva JS, Forsberg BR (2018) Influence of plankton metabolism and mixing depth on CO_2 dynamics in an Amazon floodplain lake. Sci Total Environ 630:1381–1393. https://doi.org/10.1016/j.scitotenv.2018.02.331

Amaral JHF, Melack JM, Barbosa PM, MacIntyre S, Kasper D, Cortés A, Freire Silva TS, Nunes de Sousa R, Forsberg BR (2020) Carbon dioxide fluxes to the atmosphere from waters within flooded forests in the Amazon basin. J Geophys Res Biogeosci 125:e2019JG005293. https://doi.org/10.1029/2019JG005293

American Public Health Association (1998) Standard methods for the examination of water and wastewater. APHA

Aufdenkampe AK, Mayorga E, Raymond PA, Melack JM, Doney SC, Alin SR, Aalto RE, Yoo K (2011) Riverine coupling of biogeochemical cycles between land, oceans, and atmosphere. Front Ecol Environ 9:53–60. https://doi.org/10.1890/100014

Badraghi A, Ventura M, Polo A, Borruso L, Giammarchi F, Montagnani L (2021) Soil respiration variation along an altitudinal gradient in the Italian Alps: disentangling forest structure and temperature effects. PLoS One 16:e0247893. https://doi.org/10.1371/journal.pone.0247893

Barbosa PM, Melack JM, Farjalla VF, Amaral JHF, Scofield V, Forsberg BR (2016) Diffusive methane fluxes from Negro, Solimões and Madeira rivers and fringing lakes in the Amazon basin. Limnol Oceanogr 61(S1):S221–S237. https://doi.org/10.1002/lno.10358

Barbosa PM, Melack JM, Amaral JHF, MacIntyre S, Kasper D, Cortés A, Farjalla VF, Forsberg BR (2020) Dissolved methane concentrations and fluxes to the atmosphere from a tropical floodplain lake. Biogeochemistry 148:129–151

Basso LS, Marani L, Gatti LV, Miller JB, Gloor M, Melack J, Cassol HLG, Tejada G, Domingues LG, Arai E, Sanchez AH, Corrêa SM, Anderson L, Aragão LEOC, Correia CSC, Crispim SP, Neves RAL (2021) Amazon methane budget derived from multi-year airborne observations highlights regional variations in emissions. Commun Earth Environ 2:246. https://doi.org/10.1038/s43247-021-00314-4

Bastviken D, Tranvik LJ, Downing JA, Crill PM, Enrich-Prast A (2011) Freshwater methane emissions offset the continental carbon sink. Science 331(50):2011. https://doi.org/10.1126/science.1196808

Bernhardt ES, Savoy P, Vlah MJ, Appling AP, Koenig LE, Hall RO Jr, Arroita M, Blaszczak JR, Carter AM, Cohen M, Harvey JW, Heffernan JB, Helton AM, Hosen JD, Kirk L, McDowell WH, Stanley EH, Yackulic CB, Grimm NB (2022) Light and flow regimes regulate the metabolism of rivers. Proc Natl Acad Sci USA 119:e2121976119. https://doi.org/10.1073/pnas.2121976119

Bliss A, Hock R, Radić V (2014) Global response of glacier runoff to twenty-first century climate change. J Geophys Res Earth Surf 119:717–730. https://doi.org/10.1002/2013JF002931

Bonnema M, David CH, Frasson RPM, Oaida C, Yun S-H (2022) The global surface area variations of lakes and reservoirs as seen from satellite remote sensing. Geophys Res Lett 49:e2022GL098987. https://doi.org/10.1029/2022GL098987

Borges AV, Abril G, Delille B, Descy J-P, Darchambeau F (2011) Diffusive methane emissions to the atmosphere from Lake Kivu (Eastern Africa). J Geophys Res Biogeosc 116:G03032. https://doi.org/10.1029/2011JG001673

Borges AV, Abril G, Darchambeau F, Teodoru CR, Deborde J, Vidal LO, Lambert T, Bouillon S (2015) Divergent biophysical controls of aquatic CO_2 and CH_4 in the World's two largest rivers. Sci Rep 5:15614. https://doi.org/10.1038/srep15614

Borges AV, Deirmendjian L, Bouillon S, Okello W, Lambert T, Roland FAE, Razanamahandry VF, Voarintsoa NRG, Darchambeau F, Kimirei IA, Descy J-P, Allen GH, Morana C (2022) Greenhouse gas emissions from African lakes are no longer a blind spot. Sci Adv 8(eabi8716):1–17. https://doi.org/10.1126/sciadv.abi8716

Borges AV, Okello W, Bouillon S, Deirmendjian L, Nankabirwa A, Nabafu E, Lambert T, Descy J-P, Morana C (2023) Spatial and temporal variations of dissolved CO_2, CH_4 and N_2O in Lakes Edward and George (East Africa). J Great Lakes Res 49:229–245. https://doi.org/10.1016/j.jglr.2022.11.010

Borges AV, Bouillon S, Abril G, Delille B, Poirier D, Commarieu M-V, Lepoint G, Morana C, Champenois W, Servais P, Descy J-P, Darchambeau F (2012) Variability of carbon dioxide and methane in the epilimnion of Lake Kivu. In: Descy J-P, Darchambeau F, Schmid M (eds) Lake Kivu: Limnology and biogeochemistry of a tropical great lake. Aquatic Ecology Series, Springer, pp 47–66. https://doi.org/10.1007/978-94-007-4243-7_4

Bosson JB, Huss M, Cauvy-Fraunié S, Clément JC, Costes G, Fischer M, Poulenard J, Arthaud F (2023) Future emergence of new ecosystems caused by glacial retreat. Nature 620:562–569. https://doi.org/10.1038/s41586-023-06302-2

Cardoso SJ, Enrich-Prast A, Pace ML, Roland F (2014) Do models of organic carbon mineralization extrapolate to warmer tropical sediments? Limnol Oceanogr 59:48–54

Casas-Ruiz JP, Hutchins RHS, del Giorgio PA (2021) Total aquatic carbon emissions across the boreal biome of Québec driven by watershed slope. J Geophys Res 126:e2020JG005863. https://doi.org/10.1029/2020JG005863

Chiriboga G, Borges AV (2023) Andean headwater and piedmont streams are hot spots of carbon dioxide and methane emissions in the Amazon basin. Commun Earth Environ 4:76. https://doi.org/10.1038/s43247-023-00745-1

Cohen AP, Melack JM (2020) Carbon dioxide supersaturation in high-elevation oligotrophic lakes and reservoirs in the Sierra Nevada, California. Limnol Oceanogr 65:612–626. https://doi.org/10.1002/lno.11330

Cole JJ, Caraco NF (2018) Atmospheric exchange of carbon dioxide in a low-wind oligotrophic lake measured by the addition of SF_6. Limnol Oceanogr 43:647–656. https://doi.org/10.4319/lo.1998.43.4.0647

Cole JJ (2013) Freshwater ecosystems and the carbon cycle, Excellence in Ecology Book 18, 1–142, International Ecology Institute, https://www.int-res.com/book-series/excellence-in-ecology-books/ee18/

Crawford JT, Dornblaser MM, Stanley EH, Clow DW, Striegl RG (2015) Source limitation of carbon gas emissions in high-elevation mountain streams and lakes. J Geophys Res Biogeosci 120:952–964. https://doi.org/10.1002/2014JG002861

Deemer BR, Holgerson MA (2021) Drivers of methane flux differ between lakes and reservoirs, complicating global upscaling efforts. J Geophys Res Biogeosci 126:e2019JG005600. https://doi.org/10.1029/2019JG005600

DelSontro T, Beaulieu JJ, Downing JA (2018) Greenhouse gas emissions from lakes and impoundments: Upscaling in the face of global change. Limnol Oceanogr Lett 3:64–75. https://doi.org/10.1002/lol2.10073

Dickson AG, Sabine CL, Christian JR (2007) Guide to best practices for ocean CO2 measurements. PICES Special Publication 3, 191 pp 191. https://doi.org/10.25607/OBP-1342

Fernandez JM, Townsend-Small A, Zastepa A, Watson SB, Brandes JA (2020) Methane and nitrous oxide measured throughout Lake Erie over all seasons indicate highest emissions from the eutrophic Western Basin. J Great Lakes Res 46:1604–1614. https://doi.org/10.1016/j.jglr.2020.09.011

Fick SE, Hijmans RJ (2017) WorldClim 2: new 1km spatial resolution climate surfaces for global land areas. Int J Climatol 37:4302–4315. https://doi.org/10.1002/joc.5086

Finlay K, Leavitt PR, Patoine A, Wissel B (2010) Magnitudes and controls of organic and inorganic carbon flux through a chain of hardwater, lakes on the northern Great Plains. Limnol Oceanogr 55:1551–1564. https://doi.org/10.4319/lo.2010.55.4.1551

Gillikin DP, Bouillon S (2007) Determination of δ18O of water and δ13C of dissolved inorganic carbon using a simple modification of an elemental analyzer – isotope ratio mass spectrometer (EA-IRMS): an evaluation. Rapid Comm Mass Spectrom 21:1475–1478. https://doi.org/10.1002/rcm.2968

Gran G (1952) Determination of the equivalence point in potentiometric titrations Part II. Analyst 77:661–671. https://doi.org/10.1039/AN9527700661

Grasset C, Mendonça R, Villamor Saucedo G, Bastviken D, Roland F, Sobek S (2018) Large but variable methane production in anoxic freshwater sediment upon addition of allochthonous and autochthonous organic matter. Limnol Oceanogr 63:1488–1501. https://doi.org/10.1002/lno.10786

Guo M, Zhuang Q, Tan Z, Shurpali N, Juutinen S, Kortelainen P, Martikainen PJ (2020) Rising methane emissions from boreal lakes due to increasing ice-free days. Environ Res Lett 15:064008. https://doi.org/10.1088/1748-9326/ab8254

Håkan J, Brolin AA, Håkanson L (2007) New approaches to the modelling of lake basin morphometry. Environ Model Assess 12:213–228. https://doi.org/10.1007/s10666-006-9069-z

Holgerson MA, Raymond PA (2016) Large contribution to inland water CO_2 and CH_4 emissions from very small ponds. Nat Geosci 9:222–226. https://doi.org/10.1038/ngeo2654

Hu M, Chen D, Dahlgren RA (2016) Modeling nitrous oxide emission from rivers: a global assessment. Glob Change Biol 22:3566–3582. https://doi.org/10.1111/gcb.13351

Inguaggiato S, Hidalgo S, Beate B, Bourquin J (2010) Geochemical and isotopic characterization of volcanic and geothermal fluids discharged from the Ecuadorian volcanic arc. Geofluids 10:525–541. https://doi.org/10.1111/j.1468-8123.2010.00315.x

Johnson MS, Matthews E, Du J, Genovese V, Bastviken D (2022) Methane emission from global lakes: new spatiotemporal data and observation-driven modeling of methane dynamics indicates lower emissions. J Geophys Res Biogeosci 127:e2022JG006793. https://doi.org/10.1029/2022JG006793

Junk WJ, Bayley PB, Sparks RE (1989) The flood pulse concept in river–floodplain systems. Can J Fish Aquat Sci 106:110–127

Juutinen S, Rantakari M, Kortelainen P, Huttunen JT, Larmolal T, Alm J, Silvola J, Martikainen PJ (2009) Methane dynamics in different boreal lake types. Biogeosciences 6:209–223. https://doi.org/10.5194/bg-6-209-2009

Karlsson J, Byström P, Ask J, Ask P, Persson L, Jansson M (2009) Light limitation of nutrient-poor lake ecosystems. Nature 460:506–510. https://doi.org/10.1038/nature08179

Kortelainen P, Larmola T, Rantakari M, Juutinen S, Alm J, Martikainen PJ (2020) Lakes as nitrous oxide sources in the boreal landscape. Glob Change Biol 26:1432–1445. https://doi.org/10.1111/gcb.14928

Kroeze C, Dumont E, Seitzinger SP (2010) Future trends in emissions of N_2O from rivers and estuaries. J Integr Environ Sc 7:71–78. https://doi.org/10.1080/1943815X.2010.496789

Lapierre JF, del Giorgio PA (2012) Geographical and environmental drivers of regional differences in the lake pCO_2 versus DOC relationship across northern landscapes. J Geophys Res 117:G03015. https://doi.org/10.1029/2012JG001945

Lauerwald R, Laruelle GG, Hartmann J, Ciais P, Regnier PAG (2015) Spatial patterns in CO_2 evasion from the global river network. Global Biogeochem Cycles 29:534–554. https://doi.org/10.1002/2014GB004941

Lauerwald R, Regnier P, Figueiredo V, Enrich-Prast A, Bastviken D, Lehner B, Maavara T, Raymond P (2019) Natural lakes are a minor global source of N_2O to the atmosphere. Global Biogeochem Cycles 33:1564–1581. https://doi.org/10.1029/2019GB006261

Lauerwald R, Allen GH, Deemer BR, Liu S, Maavara T, Raymond P, Alcott L, Bastviken D, Hastie A, Holgerson MA, Johnson MS, Lehner B, Lin P, Marzadri A, Ran L, Tian H, Yang X, Yao Y, Regnier P (2023) Inland water greenhouse gas budgets for RECCAP2: 1. State-of-the-art of global scale assessments. Global Biogeochem Cycles 37:e2022GB007657. https://doi.org/10.1029/2022GB007657

Lewis WM Jr (1987) Tropical limnology. Ann Rev Ecol Syst 18:159–184. https://doi.org/10.1146/annurev.es.18.110187.001111

Lewis JR (1993) Multipoint scales: Mean and median differences and observed significance levels. Int J Hum-Comput Interact 5:383–392. https://doi.org/10.1080/10447319309526075

Linke S, Lehner B, Ouellet Dallaire C, Ariwi J, Grill G, Anand M, Beames P, Burchard-Levine V, Maxwell S, Moidu H, Tan F, Thieme M (2019) Global hydro-environmental sub-basin and river reach characteristics at high spatial resolution. Sci Data 6:283. https://doi.org/10.1038/s41597-019-0300-6

Liu S, Kuhn C, Amatulli G, Aho K, Butman DE, Allen GH, Lin P, Pan M, Yamazaki D, Brinkerhoff C, Gleason C, Xia X, Raymond PA (2022) The importance of hydrology in routing terrestrial carbon to the atmosphere via global streams and rivers. Proc Natl Acad Sci USA 119(11):e2106322119. https://doi.org/10.1073/pnas.2106322119

López-Moreno JI, Fontaneda S, Bazo J, Revuelto J, Azorin-Molina C, Valero-Garcés B, Morán-Tejeda E, Vicente-Serrano SM, Zubieta R, Alejo-Cochachín J (2014) Recent glacier retreat and climate trends in Cordillera Huaytapallana, Peru. Global Planet Change 112:1–11. https://doi.org/10.1016/j.gloplacha.2013.10.010

Maavara T, Lauerwald R, Laruelle GG, Akbarzadeh Z, Bouskill NJ, Van Cappellen P, Regnier P (2019) Nitrous oxide emissions from inland waters: Are IPCC estimates too high? Glob Change Biol 25:473–448. https://doi.org/10.1111/gcb.14504

Malhi Y, Melack J, Gatti LV, Ometto J, Kesselmeier J, Wolff S, Aragão LEO, Costa M, Saleska S, Pangala SR, Basso LS, Rizzo L, Araùjo AC, Restrepo-Coupe N, Junior CHLS (2021) Chapter 6: Biogeochemical Cycles of the Amazon. In Amazon Assessment Report 2021. United Nations Sustainable Development Solutions Network, New York, USA. https://doi.org/10.55161/TAKR3454

Mandryk RR, Capelle DW, Manning CC, Tortell P, McCulloch RD, Papakyriakou T (2021) First estimation of the diffusive methane flux and concentrations from Lake Winnipeg, a large, shallow and eutrophic lake. J Great Lakes Res 47:741–750. https://doi.org/10.1016/j.jglr.2021.03.011

Marotta H, Duarte CM, Sobek S, Enrich-Prast A (2009) Large CO_2 disequilibria in tropical lakes. Global Biogeochem Cycles 23:GB4022. https://doi.org/10.1029/2008GB003434

Marzolf NS, Ardón M (2021) Ecosystem metabolism in tropical streams and rivers: a review and synthesis. Limnol Oceanogr 66:1627–1638. https://doi.org/10.1002/lno.11707

McClain ME, Naiman RJ (2008) Andean influences on the biogeochemistry and ecology of the Amazon River. Bioscience 58:325–338. https://doi.org/10.1641/B580408

McCrackin ML, Elser JJ (2011) Greenhouse gas dynamics in lakes receiving atmospheric nitrogen deposition. Global Biogeochem Cycles 25:GB4005. https://doi.org/10.1029/2010GB003897

McDonald CP, Rover JA, Stets EG, Striegl RG (2012) The regional abundance and size distribution of lakes and reservoirs in the United States and implications for estimates of global lake extent. Limnol Oceanogr 57:597–606. https://doi.org/10.4319/lo.2012.57.2.0597

Melack JM (2016) Aquatic ecosystems. In: Nagy L, Forsberg BR, Artaxo P (eds) Interactions between biosphere, atmosphere and human land use in the Amazon basin. Springer, Berlin, pp 119–148

Melack JM, Basso LS, Fleischmann AS, Botía S, Guo M, Zhou W, Barbosa PM, Amaral JHF, MacIntyre S (2022) Challenges regionalizing methane emissions using aquatic environments in the Amazon basin as examples. Front Environ Sci 10:866082. https://doi.org/10.3389/fenvs.2022.866082

Melián GV, Toulkeridis T, Pérez NM, Hernández PA, Somoza L, Padrón E, Amonte C, Alonso M, Asensio-Ramos M, Cordero M (2021) Geochemistry of water and gas emissions from Cuicocha and Quilotoa volcanic lakes. Ecuador Front Earth Sci 9:741528. https://doi.org/10.3389/feart.2021.741528

Messager ML, Lehner B, Grill G, Nedeva I, Schmitt O (2016) Estimating the volume and age of water stored in global lakes using a geo-statistical approach. Nat Commun. https://doi.org/10.1038/ncomms13603

Millero FJ (1979) The thermodynamics of the carbonate system in seawater. Geochem Cosmochem Acta 43:1651–1661. https://doi.org/10.1016/0016-7037(79)90184-4

Mitchell C, Sanders CJ, Enrich-Prast A, Sanders L, Marotta H, Santos IR, Maher DT (2018) Radon-traced pore-water as a potential source of CO_2 and CH_4 to receding black and clear water environments in the Amazon Basin. Limnol Oceanogr Lett 3:375–383. https://doi.org/10.1002/lol2.10089

Morana C, Borges AV, Deirmendjian L, Okello W, Sarmento H, Descy J-P, Kimirei IA, Bouillon S (2023) Prevalence of autotrophy in non-humic African lakes. Ecosystems 26:627–642. https://doi.org/10.1007/s10021-022-00783-4

Mosquera PV, Hampel H, Vázquez RF, Catalan J (2022) Water chemistry variation in tropical high-mountain lakes on old volcanic bedrocks. Limnol Oceanogr 67:1522–1536. https://doi.org/10.1002/lno.12099

Ngochera MJ, Bootsma HA (2020) Spatial and temporal dynamics of pCO_2 and CO_2 flux in tropical Lake Malawi. Limnol Oceanogr 65:1594–1607. https://doi.org/10.1002/lno.11408

Pace ML, Prairie YT (2005) Respiration in lakes. In: del Giorgio P, Williams P (eds) Respiration in aquatic ecosystems. Oxford, Oxford Academic. https://doi.org/10.1093/acprof:oso/9780198527084.003.0007

Pangala SR, Enrich-Prast A, Basso LS, Peixoto RB, Bastviken D, Hornibrook ERC, Gatti LV, Marotta H, Calazans LSB, Sakuragui CM, Bastos WR, Malm O, Gloor E, Miller JB, Gauci V (2017) Large emissions from floodplain trees close the Amazon methane budget. Nature 552:230–234. https://doi.org/10.1038/nature24639

Peacock M, Davidson SJ, Kothawala DN, Segersten J, Futter MN (2023) Spatial and seasonal variations in dissolved methane across a large lake. J Geophys Res Biogeosci 128:e2023JG007668. https://doi.org/10.1029/2023JG007668

Pi X, Luo Q, Feng L, Xu Y, Tang J, Liang X, Ma E, Cheng R, Fensholt R, Brandt M, Cai X, Gibson L, Liu J, Zheng C, Li W, Bryan BA (2022) Mapping global lake dynamics reveals the emerging roles of small lakes. Nat Commun 13:5777. https://doi.org/10.1038/s41467-022-33239-3

Pighini S, Ventura M, Miglietta F, Wohlfahrt G (2018) Dissolved greenhouse gas concentrations in 40 lakes in the Alpine area. Aquat Sci 80:32. https://doi.org/10.1007/s00027-018-0583-2

Pineda PAL, Bauters M, Verbeeck H, Baez S, Barthel M, Bodé S, Boeckx P (2021) Ideas and perspectives: patterns of soil CO_2, CH_4, and N_2O fluxes along an altitudinal gradient—a pilot study from an Ecuadorian neotropical montane forest. Biogeosciences 18:413–421. https://doi.org/10.5194/bg-18-413-2021

Poulenard J, Podwojewski P, Herbillon AJ (2003) Characteristics of non-allophanic Andisols with hydric properties from the Ecuadorian páramos. Geoderma 117:267–281. https://doi.org/10.1016/S0016-7061(03)00128-9

Raymond PA, Zappa CJ, Butman D, Bott TL, Potter J, Mulholland P, Laursen AE, McDowell WH, Newbold D (2012) Scaling the gas transfer velocity and hydraulic geometry in streams and small rivers. Limnol Oceanogr. https://doi.org/10.1215/21573689-1597669

Raymond PA, Hartmann J, Lauerwald R, Sobek S, McDonald C, Hoover M, Butman D, Striegl R, Mayorga E, Humborg C, Kortelainen P, Dürr H, Meybeck M, Ciais P, Guth P (2013) Global carbon dioxide emissions from inland waters. Nature 503:355–359. https://doi.org/10.1038/nature12760

Rocher-Ros G, Stanley EH, Loken LC, Casson NJ, Raymond PA, Liu S, Amatulli G, Sponseller RA (2023) Global methane emissions from rivers and streams. Nature 621:530–535. https://doi.org/10.1038/s41586-023-06344-6

Rodríguez-Cardona BM, Houle D, Couture S, Lapierre J-F, del Giorgio PA (2023) Long-term trends in carbon and color signal uneven

browning and terrestrialization of northern lakes. Commun Earth Environ 4:338. https://doi.org/10.1038/s43247-023-00999-9

Roehm CL, Prairie YT, del Giorgio PA (2009) The pCO2 dynamics in lakes in the boreal region of northern Québec, Canada. Global Biogeochem Cycles 23:GB3013. https://doi.org/10.1029/2008GB003297

Rosentreter JA, Borges AV, Deemer BR, Holgerson MA, Liu S, Song C, Melack J, Raymond PA, Duarte CM, Allen GH, Olefeldt D, Poulter B, Battin TI, Eyre BD (2021) Half of global methane emissions come from highly variable aquatic ecosystem sources. Nat Geosci 14:225–230. https://doi.org/10.1038/s41561-021-00715-2

Saunois M, Stavert AR, Poulter B, Bousquet P, Canadell JG, Jackson RB, Raymond PA, Dlugokencky EJ, Houweling S, Patra PK, Ciais P, Arora VK, Bastviken D, Bergamaschi P, Blake DR, Brailsford G, Bruhwiler L, Carlson KM, Carrol M, Castaldi S, Chandra N, Crevoisier C, Crill PM, Covey K, Curry CL, Etiope G, Frankenberg C, Gedney N, Hegglin MI, Höglund-Isaksson L, Hugelius G, Ishizawa M, Ito A, Janssens-Maenhout G, Jensen KM, Joos F, Kleinen T, Krummel PB, Langenfelds RL, Laruelle GG, Liu L, Machida T, Maksyutov S, McDonald KC, McNorton J, Miller PA, Melton JR, Morino I, Müller J, Murguia-Flores F, Naik V, Niwa Y, Noce S, O'Doherty S, Parker RJ, Peng C, Peng S, Peters GP, Prigent C, Prinn R, Ramonet M, Regnier P, Riley WJ, Rosentreter JA, Segers A, Simpson IJ, Shi H, Smith SJ, Steele PL, Thornton BF, Tian H, Tohjima Y, Tubiello FN, Tsuruta A, Viovy N, Voulgarakis A, Weber TS, van Weele M, van der Werf GR, Weiss RF, Worthy D, Wunch D, Yin Y, Yoshida Y, Zhang W, Zhang Z, Zhao Y, Zheng B, Zhu Q, Zhu Q, Zhuang Q (2020) The global methane budget: 2000–2017. Earth Syst Sci Data 12:1561–1623. https://doi.org/10.5194/essd-12-1561-2020

Sawakuchi HO, Bastviken D, Sawakuchi AO, Krusche AV, Ballester MV, Richey JE (2014) Methane emissions from Amazonian rivers and their contribution to the global methane budget. Glob Chang Biol 20:2829–2840. https://doi.org/10.1111/gcb.12646

Sawakuchi HO, Neu V, Ward ND, Barros MLC, Valerio AM, Gagne-Maynard W, Cunha AC, Less DFS, Diniz JEM, Brito DC, Krusche AV, Richey JE (2017) Carbon dioxide emissions along the lower Amazon River. Front Mar Sci 4:76. https://doi.org/10.3389/fmars.2017.00076

Seekell DA, Pace ML (2011) Does the Pareto distribution adequately describe the size-distribution of lakes? Limnol Oceanogr 56:350–356. https://doi.org/10.4319/lo.2011.56.1.0350

Seekell DA, Lapierre J-F, Ask J, Bergström A-K, Deininger A, Rodríguez P, Karlsson J (2015) The influence of dissolved organic carbon on primary production in northern lakes. Limnol Oceanogr 60:1276–1285. https://doi.org/10.1002/lno.10096

Sikder MS, Wang J, Allen GH, Sheng Y, Yamazaki D, Song C, Ding M, Crétaux J-F, Pavelsky TM (2023) Lake-TopoCat: a global lake drainage topology and catchment database. Earth Syst Sci Data 15:3483–3511. https://doi.org/10.5194/essd-15-3483-2023

Sobek S, Tranvik LJ, Cole JJ (2005) Temperature independence of carbon dioxide supersaturation in global lakes. Global Biogeochem Cycles 19:GB2003. https://doi.org/10.1029/2004GB002264

Staehr PA, Baastrup-Spohr L, Sand-Jensen K, Stedmon C (2012) Lake metabolism scales with lake morphometry and catchment conditions. Aquat Sci 74:155–169. https://doi.org/10.1007/s00027-011-0207-6

Stallard RF (1998) Terrestrial sedimentation and the carbon cycle: coupling weathering and erosion to carbon burial. Global Biogeochem Cycles 12:231–257. https://doi.org/10.1029/98GB00741

Standing committee of Analysts (1981) Ammonia in waters. Methods for the examination of waters and associated materials. 16 pp (HMSO, 1981)

Toming K, Kotta J, Uuemaa E, Sobek S, Kutser T, Tranvik LJ (2020) Predicting lake dissolved organic carbon at a global scale. Sci Rep 10:8471. https://doi.org/10.1038/s41598-020-65010-3

Wang L, Xiao C-D, Du Z-H, Maher DT, Liu J-F, Wei Z-Q (2022) In-situ measurement on air–water flux of CH_4, CO_2 and their carbon stable isotope in lakes of northeast Tibetan Plateau. Adv Clim Change Res 13:279–289. https://doi.org/10.1016/j.accre.2022.02.001

Wanninkhof R (1992) Relationship between wind speed and gas exchange over the ocean. J Geophys Res 97:7373–7382. https://doi.org/10.1029/92JC00188

Weiss RF (1981) Determinations of carbon dioxide and methane by dual catalyst flame ionization chromatography and nitrous oxide by electron capture chromatography. J Chromatogr Sci 19:611–616. https://doi.org/10.1093/chromsci/19.12.611

Weiss RF, Price BA (1980) Nitrous oxide solubility in water and seawater. Mar Chem 8:347–359. https://doi.org/10.1016/0304-4203(80)90024-9

Wilson C, Gloor M, Gatti LV, Miller JB, Monks SA, McNorton J, Bloom AA, Basso LS, Chipperfield MP (2016) Contribution of regional sources to atmospheric methane over the Amazon Basin in 2010 and 2011. Glob Biogeochem Cycles 30:400–420. https://doi.org/10.1002/2015GB005300

Wilson C, Chipperfield MP, Gloor M, Parker RJ, Boesch H, McNorton J, Gatti LV, Miller JB, Basso LS, Monks SA (2021) Large and increasing methane emissions from eastern Amazonia derived from satellite data, 2010–2018. Atmos Chem Phys 21:10643–10669. https://doi.org/10.5194/acp-21-10643-2021

Yan F, Sillanpää M, Kang S, Aho KS, Qu B, Wei D, Li X, Li C, Raymond PA (2018) Lakes on the Tibetan Plateau as conduits of greenhouse gases to the atmosphere. J Geophys Res Biogeosci 123:2091–2103. https://doi.org/10.1029/2017JG004379

Yan F, Du Z, Pu T, Xu Q, Wang L, Ma R, Zhang C, Yu Z, Li C, Kang S (2023) Isotopic composition and emission characteristics of CO_2 and CH_4 in glacial lakes of the Tibetan Plateau. Environ Res Lett 18:094025. https://doi.org/10.1088/1748-9326/aceb7b

Yvon-Durocher G, Allen AP, Bastviken D, Conrad R, Gudasz C, St-Pierre A, Thanh-Duc N, del Giorgio PA (2014) Methane fluxes show consistent temperature dependence across microbial to ecosystem scales. Nature 507:488–491. https://doi.org/10.1038/nature13164

Zapata A, Rivera-Rondón CA, Valoyes D, Muñoz-López CL, Mejía-Rocha M, Catalan J (2021) Páramo lakes of Colombia: An overview of their geographical distribution and physicochemical characteristics. Water 13:2175. https://doi.org/10.3390/w13162175